ISSN 0801–9940
ISBN 82–553–1149–1

No. 98 - 1

Application of the Perturbation Method to Plate Buckling Problems

by

Eivind Steen

RESEARCH REPORT IN MECHANICS

UNIVERSITY OF OSLO
DEPARTMENT OF MATHEMATICS
MECHANICS DIVISION

1998

UNIVERSITETET I OSLO
MATEMATISK INSTITUTT
AVDELING FOR MEKANIKK

Application of the Perturbation Method to Plate Buckling Problems

EIVIND STEEN

Mechanics Division, Department of Mathematics, University of Oslo

Abstract - The perturbation method is applied in an incremental scheme for tracing non-linear equilibrium paths of structures which are subjected to a set of simultaneously acting external loads. The method is based on the discretesized version of the non-linear stability theory and it is used for solving non-linear algebraic equations. In order to pass limit points the direct arc length concept is introduced. The method is especially adapted to the solution of plate buckling problems for which both strength and in-plane stiffness properties are important parameters. As an example the perturbation procedure was used for solving a simple plate buckling problem, for which a closed form solution exist, and the results were compared against a recognised non-linear finite element program.

TABLE OF CONTENTS

1. INTRODUCTION

The most significant contribution within the field of non-linear buckling theory of structures was the development made by Koiter (1945) and first presented in his classical thesis of 1945. He classified the postbuckling behaviour according to the stability of the critical load itself, and introduced useful concepts for postbuckling and imperfection sensitivity. Two decades later, in the beginning of the sixties, Budiansky and Hutchinson (1964) developed this theory further. The theory was subsequently applied to several shell buckling problems (Hutchinson 1967, Budiansky and Amazigo 1968, Hutchinson 1968, Budiansky 1969). Budiansky (1974) has provided a comprehensive summary of the theory.

The basis for this non-linear buckling theory is the application of perturbation methods by which the equilibrium curve in the postbuckling range is approximated as a power series expanded around the critical load. For unstable structures, which could be analysed with sufficient accuracy with one single degree of freedom, the buckling capacity of a geometrically imperfect structure was related to the imperfection amplitude through very compact and practical formulas. A comprehensive review of the theory is given by Hutchinson and Koiter (1970).

A parallel development of a more general non-linear buckling theory was initiated in the U.K. in the beginning of the sixties. These theories by Sewell (1965,1968), Thompson (1965), Thompson and Hunt (1973), Huseyin (1975) and others were based on a discretized version of structural non-linear theories and the static perturbation method was introduced for explicit solutions of the postbuckling behaviour. Chilver (1967), Johns (1971), Supple (1967) and others have studied structural models with several degrees of freedom for the identification and classification of coupled postbuckling paths. Thompson and Hunt (1984) developed the procedure further and made analogies to catastrophe theory.

The general Koiter theory have been used by several authors with the purpose of calculating buckling strength of thin-walled plate and shell structures. Notable among these are Benito and Sridharan (1985), van Erp and Menken (1991) and Lanco and Garcea (1996). All these applications can be classified as asymptotic in the sense that they are based on a Taylor expansion around the critical state.

The more traditional approach, used in commercial finite element programs, is to solve the structural problem using an incremental solution procedure. The literature on this type of numerical analysis is very extensive and within the engineering field, the first publications emerged in the early sixties in connection with the development of the finite element method. It is not the purpose to review this topic here but it can be stated that Riks (1972, 1979) were among the first to formulate the arc length concept for passing limit points. The Riks method has been recognised as a powerful strategy and more recent reviews of this numerical technique can be found in Crisfield and Shi (1991) and Carrera (1994). Stoll (1994) applied the Riks method for the detailed study of the snap phenomenon in buckled plates.

The motivation for the present work has been on different levels. First of all it is has been the purpose to explore the possibilities of the perturbation method as a numerical tool for solving structural stability problems within the field of thin-walled plate and shell structures. The Koiter theory, as described by the different authors referenced above, is the obvious example

of such an application. However, these applications are constructed with the main purpose of exploring the postbuckling behaviour around a critical point, which is normally to be understood as the classical buckling load. Since the perturbation method is based on a power series expansion, these analyses are only valid in the close vicinity of the critical point itself. This is a serious restriction to their practical usefulness.

However, it is obvious that the perturbation method can be used also in an incremental scheme, in which the total equilibrium path from the unloaded state to an advanced postbuckled state can be followed. Such an application is explored herein and the present author is not familiar with similar applications of the perturbation method in the literature.

The perturbation method is used as a tool for solving algebraic non-linear equations. The procedure of discretization of the structural problem, which generates the algebraic equations, can be chosen as matter of personal preference or more wisely as function of the actual problem in hand. For some problems the finite element method is to be preferred while for other problems a Rayleigh-Ritz technique based on a Fourier expansion of the deflections may be a more efficient choice. The perturbation method as a numerical tool is equally applicable.

The procedure herein is restricted to the study of what is often referred to as an imperfect system. This means briefly that geometrical imperfections are added in all degrees of freedom and buckling deflections will start to grow from the onset of applied loading. Conceptually thus only limit point buckling is handled and bifurcation type of buckling is suppressed. The main field of application of the proposed perturbation procedure is seen within the field of the development of simplified buckling models. This means buckling models with a limited number of degrees of freedom and which describes the structural response with sufficient accuracy for design purposes. Thus, the procedure described herein is not developed to a level that makes it competitive with full blown non-linear finite element programs. In order to provide this, stability and bifurcation buckling criteria have to be included. Such criteria are readily available within the field of perturbation methods as part of the study of singular solutions, but they are not explored herein.

Within the field of ship and offshore constructions, which are mainly constructed of thin walled stiffened plates and shells, the existing design methods are very simplified and very often based on crude empirical approximations. With the steady development of the personal computers more and more of the analyses of such structures are done by numerical tools, typically large linear finite element models. Thus a need emerge that facilitates strength assessment procedures which match the detailed information of the actual stress flow in the structure. The motivation for applying crude formulas for strength control is reduced and it may be material to be saved and safety to be gained by using more advanced design methods. From this perspective it lies a motivation for applying more advanced buckling check procedures of plates and shells.

It has been the purpose herein to focus on strength and stiffness properties of plates, which is seen as the basic units in large ship and offshore structures. By using a Rayleigh-Ritz disctretization of deflections in terms of Fourier expansions, the buckling behaviour of plates can be described by sufficient accuracy using only some few degrees of freedom and the computer time to assess the strength is minimal. The buckled plate can be considered as

macro material in an overall sense and it is believed that the perturbation procedure provides an improved understanding of the concepts of buckling, postbuckling and imperfection sensitivity.

With this as the motivation, the present report starts in Chapter 2 with a general description of the perturbation method and some of the basic concepts used in the general non-linear stability theory are illustrated. For structural problems with multiply acting independent loads the concept of equilibrium surface is central. Chaper 2 focuses on the study of the mathematical local shape of the equilibrium surface and it is shown how the perturbation method provides this information. Chapter 2 starts with a presentation of the standard load or displacement control procedures, and it is shown how these fail to predict snap buckling behaviour. The direct arc length concept is then introduced as a method for solving these problems. In a mathematical language this means a numerical strategy with capability to pass folds and limit points on the equilibrium surface. The perturbation procedure calculates the local shape of the equilibrium surface and the application of these properties is further discussed in Chapter 3 in connection stiffness properties of the structure. Within geometrically non-linear plate theory it is shown how the perturbation procedure provides directly the coefficients to be used in the assessment of the instaneous plate stiffness properties. The concept of the macro material is introduced.

The perturbation procedure together with the direct arc length concept provides the path derivatives in the direction of the prescribed load path. These path derivatives, used in an incremental procedure, are used directly for tracing the equilibrium curve. As a post-calculation feature, the associated multiple path derivatives in each state along this curve can be assessed. This gives the directional stiffness coefficients for the structure in all load directions. The first order directional stiffness coefficients calculated from the perturbation procedure are the same as the tangent stiffness matrix coefficients used in traditional solution procedures, which connect the incremental external loads to the corresponding incremental deflections.

In Chapter 4 an unstiffened plate subjected to biaxial in-plane loads is analysed as an example. Only one term is used in the Rayleigh-Ritz discretization of the out-of plane deflection and, through the use of compatibility conditions between out-of plane and in-plane deflections, a single degree of freedom model is derived. This gives a closed form solution which is compared against the perturbation method used in an incremental scheme and comparisons with numerical results using the recognised non-linear finite element program ABAQUS (1994) is also included. The example is solved using both load and displacement control, since this single degree of freedom model does not possess snap buckling features. The closed form solution, in terms of the macro material coefficients, are calculated and compared against the numerical results.

As a continuation of the study reported herein, a more extensive plate buckling model is developed for stiffened plates in Steen (1999). That model is based on a generalisation of the Shanley model concept and the emphasis is on the interaction between what is defined as local buckling modes and overall buckling. It is shown how the interaction of buckling modes leads to unstable postbuckling behaviour and it is demonstrated that the perturbation method, used in an incremental scheme with the arc length as control parameter, is able to pass the sharp peaks and limit points in load-deflection space.

The methods developed herein assume the existence of a set non-linear algebraic equilibrium equations on total form, and as such the presented procedure is based on material characteristics according to Hooke's law. The case of a non-linear elastic-plastic material characteristic requires a virtual work formulation in general. This type of behaviour is not considered in this report, but such an application, using the perturbation procedure in an incremental scheme, can be found in Steen and Andreassen (1995-I, 1995–II).

Tensor notation with the standard summation convention is used for the most part. However, vector symbols are also introduced when found convenient.

2. DESCRIPTION OF THE PERTURBATION METHOD FOR MULTIPLE LOADS

2.1 General

As mentioned in the introduction there exist many methods for solving non-linear equations and the choice of the most optimal is to a large degree a matter of personal preference. In the present work the perturbation method, introduced in the non-linear discrete stability theory by researchers such as Sewell, Thompsen, Huseyin and others, has been applied. The present exposition is meant only as an introduction to the method and a readable full account of the theory in the context of multiple loads can be found in the book by Huseyin (1975).

The present application of the perturbation procedure is used for tracing smooth equilibrium paths. This means that bifurcation buckling is avoided by considering an imperfect structural system adding geometrical imperfections in all degrees of freedom. The study of critical points in general, as part of the study of singular solutions of the perturbation procedure, is not addressed in the present work.

The perturbation method is a very systematic procedure and it gives sets of linear equations to be solved. The unknowns in the procedure are the rate of change of the deflection parameters, i.e. that is the first order rate of change, second order rate of change etc. of the deflection parameters. The rate of change is defined with respect to some chosen perturbation parameter. The clue in an automated calculation procedure is that the perturbation parameter must be chosen in such a way that it is always continuously increasing along the specified load path. This is discussed in more detail below.

The rate of the deflection parameters or of any other state variable are called path derivatives and as soon as these are known the incremental deflection from the known equilibrium point to the next can be found using the power series expansion principle. In more standard numerical schemes, such as Newton-Raphson, the incremental deflections are directly the unknowns in the procedure and not the rates of deflections. This is discussed more in detail under Section 2.3.

The needed number of terms in a perturbation expansion in a practical case will be an issue for discussion. In the present work the expansion has not been carried out further than to the second order which means that the curvature of the equilibrium path is evaluated. This is the

level of expansion used in the Koiter theory, and together with sufficiently small increments of the perturbation parameter, this will be a reasonable approximation. Compared to standard incremental schemes, the second order perturbation expansion can be interpreted as a substitute for the equilibrium control used in traditional Newton-Raphson iterations on the total equilibrium equations.

The selection of the perturbation parameters is also an important issue in the context of solution algorithms. The most convenient choice will be to select a pure load or displacement control, as this will give the simplest sets of equations. However, to choose load or displacement control in an actual case needs some qualified knowledge of the expected non-linear response of the problem in hand.

The normal conception of load or displacement control is that the respective parameter is used as a control variable. This means, say for load control, that the loads are incremented along the prescribed load path and the corresponding deflections are calculated. However, in a perturbation approach the chosen control variable have to be continuously increasing along the prescribed load path. Obviously, say for a buckling problem, the load is not a proper control parameter since the load will reach a maximum value for then to unload. This will give a singular case at the maximum load point and load control will not work for the purpose of identifying the buckling load. Exactly the same arguments can be followed in the case of displacement control. Displacement control will normally succeed in identifying the buckling load, but may fail to trace the subsequent equilibrium path due to possible snap back deflections (deflections have to be reduced in order to achieve equilibrium).

To overcome such problems the direct arc length method is introduced. The arc length method, in the context of the perturbation procedure, gives large flexibility as it can be combined with any prescribed path in the load space or displacement space. For example in standard buckling analysis it will be normal to specify a set of simultaneously acting loads. The arc length method then follows the specified route in load space until it ends up at this specified load point. If the load point is outside the buckling boundary the procedure identifies the point along the specified load path that corresponds to buckling and it will try to reach the specified load point in an advanced postbuckled state if it exists.

For the purpose of illustrating some of the problems to be encountered in the solution of a non-linear stability problem the pure load or displacement control cases are presented in Section 2.2. This description is meant as an introduction to the perturbation procedure and it shows how the load or displacement variables fail as efficient perturbation parameters. The equations up to second order are derived which provides the solution of the corresponding path derivatives. These path derivatives, valid for multiple loads are informing about the local shape of the equilibrium surfaces in all directions around any specified point. These multiple directional path derivatives are interesting in the sense that they assess the rate of growth of each deflection coefficient q_i with respect to a unit change of the different loads. They are used as parameters in the assessment of the instaneous stiffness coefficients as explained more in detail in Chapter 3.

In Section 2.3 the multiple directional path derivatives are derived in the context of the multidimensional arc length concept. This is the general approach, which have to be used unless a load or displacement control is known a priori to give a stable solution for the

problem in hand. Since the independent perturbation parameters are chosen as the arc length coordinates along the equilibrium surface, the corresponding multiple directional path derivatives may have little direct interest as they are hard to connect to any physical understanding. However, they can be used as parameters for assessing the more familiar directional stiffness coefficients of the structure. It is worth noting that the first order directional stiffness coefficients are the same as the tangent stiffness matrix coefficients used in traditional Newton-Raphson type of incremental solution procedures.

For multiple loads it is necessary to define a load path in load space or displacement space, whichever is the most relevant for the problem in hand. This is explained in Section 2.4 and it is shown how the problem will be reduced from a multiple load case to a single load case as soon as the path in load or displacement space is specified. Further, based on the direct arc length concept and a single load parameter, linear equations for the first order and second order path directed derivatives are derived. This provides the necessary information for finding the displaced structural configuration as it changes along the prescribed load path.

Section 2.5 gives an overview of the total calculation procedure seen as an incremental scheme for tracing non-linear equilibrium paths with the purpose of both identifying maximum load bearing capacity and as a procedure for assessing the current instaneous stiffness properties along the equilibrium path.

The general problem to be considered is stiffened plates subjected to a combination of multiple loads, Fig.1. Simultaneously acting loads on a stiffened plate element in a marine structure are:

i) axial compression/tension (in direction of stiffeners)
ii) transverse compression/tension (in direction normal to stiffeners)
iii) in-plane moment at edges x_1 = const.
iv) in-plane moment at edges x_2 = const.
v) in-plane shear loads
vi) lateral pressure, acting normal to the plate plane

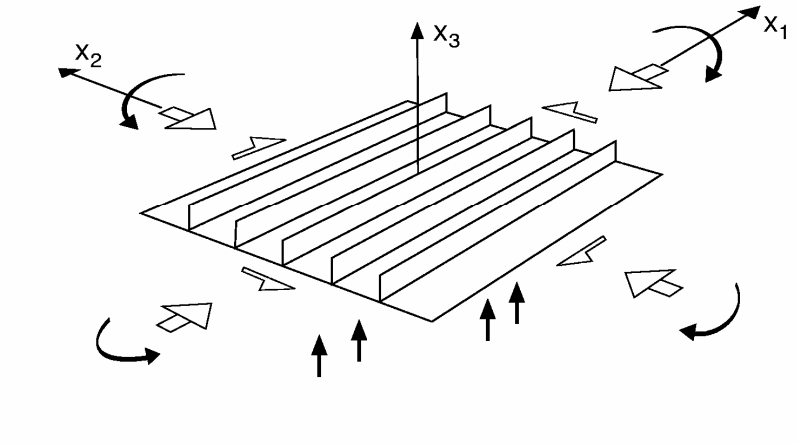

Fig.1 Multiple loads acting on a stiffened plate

Several symbols are adopted that, for convenience, are given a rather generalised meaning. It is helpful to define the following ones a priori:

q_i with i = 1,2,..., M, represents the displaced configuration of the structure and M is the total degrees of freedom. The q_i represent the displacement vector.

Λ_α with α = 1,2,..., K, represents physical loads (axial, transverse, shear, lateral pressure etc.).

Δ_α with α = 1,2,...,K, represents in-plane end-shortenings of plate edges.

All of these parameters will normally be given a non-dimensional form in specific examples.

2.2 Load or displacement control

For the purpose of illustrating important aspects that need to be accounted for in a general solution strategy, it is useful to start with a discussion of the standard load control and displacement control cases.

For the multiply loaded stiffened plate problem with K independent loads Λ_α acting, the structural theory provides M equilibrium equations. These equations may have been obtained by finite element discretizations, Rayleigh-Ritz technique or any other preferred procedure for transforming the continuos structural problem to its disctretized counterpart. The resulting equilibrium equations may be written in the following form

$$f_i(q_j, \Lambda_\alpha) = 0 \qquad i, j = 1,2,...,M;\ \alpha = 1,2,...,K \tag{1}$$

The solution of eq.(1) is written in parametric form as

$$q_i = q_i(\Lambda_\alpha) \qquad i = 1,2,...,M;\quad \alpha = 1,2,...,K \tag{2}$$

If a solution in the total form of eq.(2) was available it would imply that, for a set of prescribed loads, the deflected configuration of the structure is directly assessed and thus it follows that stress and strains in any point in the structure as function of loads could be calculated. However, such closed form solutions are not available in general and it is necessary to resort to a numerical solution strategy.

In the form of eq.(2), the loads Λ_α are used as the control parameters, i.e. the loads are chosen as the perturbation parameters. Eq.(2) may be interpreted as an equilibrium surface in the M+K dimensional space as illustrated in Fig.2. The solution expanded around a known point I_s (representing any loaded state or the unloaded state) becomes

$$q_i = q_{i,s} + q_i^{\ \alpha}(\Lambda_\alpha - \Lambda_{\alpha,s}) + \frac{1}{2!} q_i^{\ \alpha\beta}(\Lambda_\alpha - \Lambda_{\alpha,s})(\Lambda_\beta - \Lambda_{\beta,s}) + \cdots \tag{3}$$

A Greek superscript on the q_i parameters indicates partial differentiation with respect to the corresponding load variable. A subscript s indicates that the variable is evaluated at an

arbitrarily equilibrium state I_s. A necessary requirement for the path derivatives q_i^{α} and $q_i^{\alpha\beta}$ etc. to have a unique solution is that the functions, eq.(2), are single valued around any point I_s on the equilibrium surfaces, Fig.2. The left sketch in Fig.2 indicates a single valued function, which implies that the load parameters will work satisfactory as perturbation parameters. A practical example of such a case will be an unstiffened plate subjected to a normal pressure. The right sketch in Fig.2 indicates a multiply valued function, which implies that the load parameters could not be used as perturbation parameters. This represents the general case of a buckling problem in which the loads reach some upper limit load (stability or buckling boundary) for then to unload.

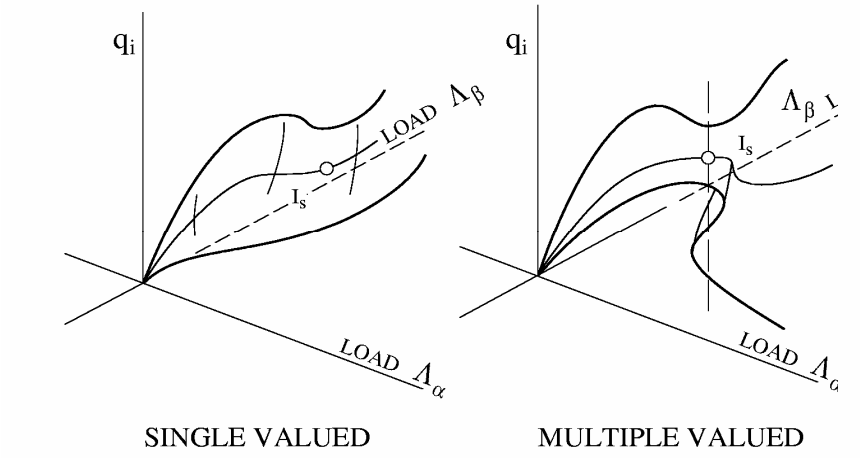

Fig. 2 Equilibrium surface under multiple loads Λ_α , Λ_β etc.

Under load control, snap buckling to an advanced stable equilibrium state, associated with a large change in deflected form, may take place. This snap will be dynamic and may be very violent. The simplest case illustrating such behaviour is the classical arc problem given in standard textbooks in structural mechanics.

Alternatively, instead of loads, it would be natural to choose the in-plane edge displacements (end-shortenings Δ_α) as the control parameters. The equilibrium equations are then transformed to

$$f_i(q_j, \Delta_\alpha) = 0 \qquad i, j = 1,2,...,M; \;\; \alpha = 1,2,...,K \tag{4}$$

with a solution in the parametric form as

$$q_i = q_i(\Delta_\alpha) \tag{5}$$

This solution may be interpreted as an equilibrium surface in the space as illustrated in Fig.2 but now with the displacements Δ_α as parameters on the horizontal axes instead of the loads Λ_α. In particular the right sketch in Fig.2 can be used as illustration of any general situation of multiple valued equilibrium surface since the horizontal axes can be interpreted as loads,

displacements or in principle any chosen set of control parameters. The solution of eq.(5) expanded around a known state I_s becomes

$$q_i = q_{i,s} + q_i{}^{\alpha}(\Delta_\alpha - \Delta_{\alpha,s}) + \frac{1}{2!}q_i{}^{\alpha\beta}(\Delta_\alpha - \Delta_{\alpha,s})(\Delta_\beta - \Delta_{\beta,s}) + \cdots \qquad (6)$$

In order to find the path derivatives, which is now defined as the rate of change with respect to the displacements Δ_α and not the loads Λ_α, eq.(5) is substituted back into eq.(4) to give

$$f_i(q_j(\Delta_\alpha), \Delta_\alpha) = 0 \qquad i, j = 1,2,...,M; \qquad \alpha = 1,2,...,K \qquad (7)$$

Partial differentiation of eq.(7) with respect to any Δ_α gives the following set of linear equations in terms of the unknown first order path derivatives $q_i{}^{\alpha}$

$$f_i{}^{j} q_j{}^{\alpha} + f_i{}^{\alpha} = 0 \qquad i, j = 1,2,...,M; \qquad \alpha = 1,2,...,K \qquad (8)$$

The $f_i{}^{j}$ is used as a symbol for the partial differentiation of the function f_i with respect to any displacement parameter q_j, and $f_i{}^{\alpha}$ is used a symbol for the partial differentiation of the function f_i with respect to any control parameter Δ_α (or Λ_α).

Similarly, second order differentiation of eq.(7) gives the following set of linear equations in terms of the unknown second order path derivatives $q_i{}^{\alpha\beta}$

$$f_i{}^{jk} q_j{}^{\alpha} q_k{}^{\beta} + f_i{}^{j} q_j{}^{\alpha\beta} + f_i{}^{j\alpha} q_j{}^{\beta} + f_i{}^{\alpha\beta} = 0 \qquad i, j, k = 1,2,...,M; \qquad \alpha,\beta = 1,2,...,K \quad (9)$$

The solution of these sets of linear equations, in terms of the first order path derivatives $q_i{}^{\alpha}$, second order path derivatives $q_i{}^{\alpha\beta}$ etc., gives parameters that describe the local form of the equilibrium surface in all directions in the close vicinity of an arbitrary state I_s. The actual state enters the problem through the load dependent coefficients $f_i{}^{j}$, $f_i{}^{\alpha}$ etc. since these coefficients are functions of the actual q_i and Δ_α values representative for a state I_s. In order to determine the actual states of interest in a practical case, the loading path in load or displacement space has to be specified. A fixed load path will in practice always start from the unloaded state and this implies that the travel route along the equilibrium surfaces may take forms as illustrated schematically in Fig.2. The specification of arbitrarily load paths is discussed more in detail in Section 2.4.

From this presentation it is illustrated that neither the loads nor the displacements are suited as control parameters due to the possibility of a multiple valued equilibrium surface which will give snap buckling problems. Load or displacement control may be used in special cases for which there is no chance of snap buckling. Lateral pressure loads on a flat unstiffened plate is such a case. Thus, in the general case alternative methods are needed and this leads to the introduction of the arc length concept described next in Section 2.3.

2.3 Direct arc length method

In view of the problems identified above, it is obvious that a very general strategy is needed to trace solutions in the general case of several simultaneously acting physical loads. One of the pioneers in the development of the perturbation method was Sewell. He published a series of papers in the late sixties and the beginning of the seventies treating all aspects of postbuckling behaviour of general non-linear systems. His approach is rather mathematical and beyond the level of the present application. However, he was among the first to apply a definition of the independent perturbation parameter as a ray in the load-deflection space with a fixed direction, Sewell(1968). The most convenient direction for obtaining solutions was proposed to be the direction of the tangent to the equilibrium curve. Thus Sewell used the same strategy as proposed at later stage by Riks (1979). Riks called this approach the arc length method and many researchers have applied this concept successfully in connection with incremental numerical Newton-Raphson type of procedures.

To our knowledge no one has applied the concept of arc length, within an incremental perturbation scheme, for solution of stability problems of structures. The purpose of such a procedure is to trace equilibrium paths across a general equilibrium surface with folds and limit points, and to assess the buckling boundaries together with the instaneous stiffness properties. Since the arc length method was first proposed within the field of perturbation methods of non-linear systems, it is pertinent to try to use it within this field also in a setting that can be a viewed as an engineering oriented approach.

In a system with M independent deflection parameters q_i and K independent load parameters Λ_α (or deflection parameters Δ_α) it is assumed that there may be defined K independent perturbation parameters η_α such that the solution to eq.(1) is always single valued and can be expressed in the parametric form

$$\begin{aligned} q_i &= q_i(\eta_\alpha) \\ \Lambda_\beta &= \Lambda_\beta(\eta_\alpha) \end{aligned} \qquad i = 1,2,...,M; \quad \alpha, \beta, \gamma = 1,2,..., K \tag{10}$$

Eq.(10) expanded around an arbitrary equilibrium state I_s gives

$$\begin{aligned} q_i &= q_{i,s} + q_i{}^{\alpha}(\eta_\alpha - \eta_{\alpha,s}) + \frac{1}{2!} q_i{}^{\alpha\beta}(\eta_\alpha - \eta_{\alpha,s})(\eta_\beta - \eta_{\beta,s}) + \cdots \\ \Lambda_\beta &= \Lambda_{\beta,s} + \Lambda_\beta{}^{\alpha}(\eta_\alpha - \eta_{\alpha,s}) + \frac{1}{2!} \Lambda_\beta{}^{\alpha\gamma}(\eta_\alpha - \eta_{\alpha,s})(\eta_\gamma - \eta_{\gamma,s}) + \cdots \end{aligned} \tag{11}$$

As before, a Greek superscript α on the q_i and Λ_β indicates partial differentiation with respect to the corresponding perturbation parameter η_α etc. A subscript s indicates that the parameter is evaluated at state I_s. The η_α parameters are to be chosen such as to ensure single valued solutions around the known point I_s. From the general shape of the equilibrium surfaces with folds etc., it will be appropriate to adopt a multi dimensional arc length concept where the η_α parameters are curvilinear coordinates following the curved equilibrium surface. We can then imagine that the concept of using the curvilinear coordinates as control parameters will map

the folded multiple valued surface of Fig.2 (right sketch) to the left sketch with the curvilinear coordinates $\eta_1, \eta_2, \ldots$ etc. being stretched out as rectangular coordinates.

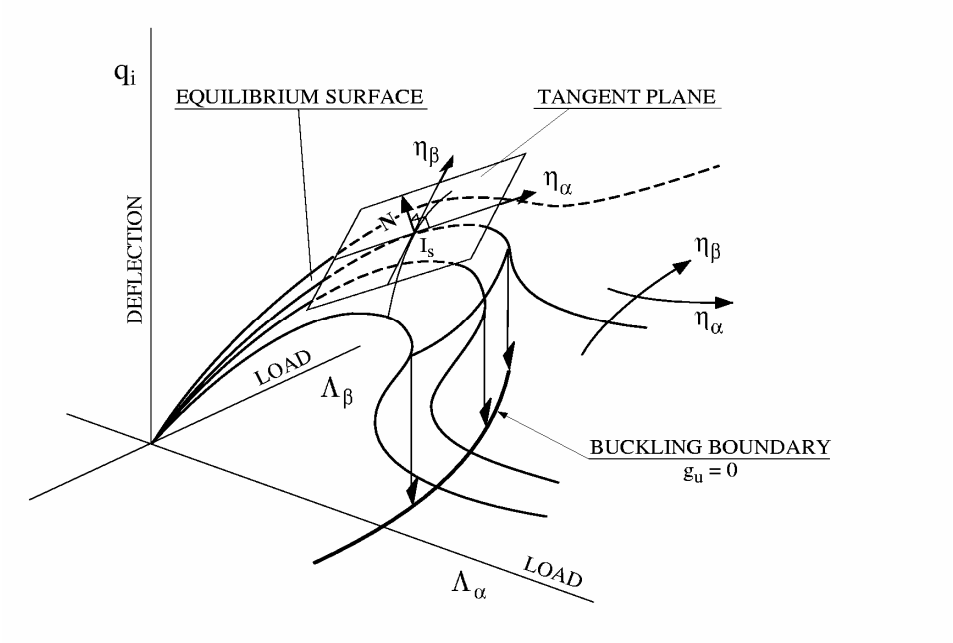

Fig.3 Curvilinear coordinates η_α following the equilibrium surface

Substituting the parametric solution of eq.(10) into eq.(1) gives

$$f_i(q_j(\eta_\alpha), \Lambda_\beta(\eta_\alpha)) = 0 \qquad i, j = 1,2,...,M;\ \alpha,\beta = 1,2,...,K \qquad (12)$$

Differentiate eq.(12) once with respect to one η_α gives

$$f_i{}^j q_j{}^\alpha + f_i{}^\beta \Lambda_\beta{}^\alpha = 0 \qquad i, j = 1,2,...,M;\ \alpha, \beta,= 1,2,...,K \qquad (13)$$

Here is per definition $f_i{}^j \equiv \partial f_i / \partial q_j$, $f_i{}^\beta \equiv \partial f_i / \partial \eta_\beta$, $q_i{}^\alpha \equiv \partial q_i / \partial \eta_\alpha$ and $\Lambda_\beta{}^\alpha \equiv \partial \Lambda_\beta / \partial \eta_\alpha$. Eq.(13) represent M*K linear equations in the total M*K+K*K unknowns $q_j{}^\alpha, \Lambda_\beta{}^\alpha$. Thus there is K*K equations lacking in order to be able to solve this first order problem. These equations are provided through the definition of the K independent perturbation parameters.

The definition of a set of efficient general perturbation parameters is very important in order to pass limit points and folds on the equilibrium surface. An intuitive approach will be to use a set of parameters that describe the tangential directions to the equilibrium surface in a known point I_s. Then by expanding the solution to the first, second or higher degree with the tangential directions as coordinates and by specifying small increments along these tangents, the neighbouring equilibrium points can be can be found. The tangents can be considered as following a set of curvilinear coordinates η_α at I_s , Fig.3. This approach is a generalisation of the arc length concept introduced by Sewell (1968) within the field of perturbation theory, as

it considers K independent load parameters instead of one. When a load path in load space or displacement space is defined the multiple load specification resembles the single load case as explained more in detail in Section 2.4.

Let us assume that a set of K coordinates η_α follows the equilibrium surface. From differential geometry (e.g. Wempner, 1973) this is the same as viewing eq.(10) as a K dimensional surface in the M+K dimensional rectangular space in terms of a set of K curvilinear coordinates η_α, Fig.3. Then we implicitly assume the existence of functions in the form

$$\begin{aligned} q_i &= q_i(\eta_1, \eta_2, ..., \eta_K) \\ \Lambda_\beta &= \Lambda_\beta(\eta_1, \eta_2, ..., \eta_K) \end{aligned} \qquad i = 1,2,...,M; \quad \alpha, \beta, \gamma = 1,2,..., K \qquad (14)$$

Assuming now that one of the curvilinear coordinate, say η_1, represent a continuous curve along the equilibrium surface with start in origin. Moreover, assuming that the coordinate along this curve describes the arc length across the equilibrium surface, we know that the first order rate of change of the position vector (measured from origin to a point I_s on the surface) along this curve is a unit tangent vector, say $\mathbf{i}_1$. From mathematics we have that the tangential ray in this point can be expressed as

$$(\eta_1 - \eta_{1,s}) = c_i{}^1(q_i - q_{i,s}) + c_\beta{}^1(\Lambda_\beta - \Lambda_{\beta,s}) \qquad (15)$$

Here $(\eta_1 - \eta_{1,s})$ are the incremental coordinate in the direction of the tangent $\mathbf{i}_1$ and $(q_i - q_{i,s})$ and $(\Lambda_\beta - \Lambda_{\beta,s})$ represent incremental coordinates along the respective rectangular axes. The $c_i{}^1$ and $c_\beta{}^1$ coefficients are the corresponding direction cosines between the unit tangent $\mathbf{i}_1$ and the respective rectangular axes. Since the directional cosines are the same as the first order path derivatives of a parametric representation of a curve in space, it is a very intuitive approach to define the tangential direction to be the independent coordinate.

From this it follows that a multidimensional set of incremental coordinates along the corresponding tangential direction is defined as

$$\eta_\alpha - \eta_{\alpha,s} = q_i{}^\alpha(q_i - q_{i,s}) + \Lambda_\beta{}^\alpha(\Lambda_\beta - \Lambda_{\beta,s}) \qquad (16)$$

where we have used the following notation

$$\begin{aligned} c_i{}^\alpha &\equiv q_i{}^\alpha \\ c_\beta{}^\alpha &\equiv \Lambda_\beta{}^\alpha \end{aligned} \qquad (17)$$

By requiring additionally that the curvilinear coordinates η_α constitutes an orthogonal set, the first order differentiation of eq.(16), with respect to some η_γ, gives the following set of equations

$$q_i{}^\alpha q_i{}^\gamma + \Lambda_\beta{}^\alpha \Lambda_\beta{}^\gamma = \delta^{\alpha\gamma} \qquad (18)$$

The $\delta^{\alpha\gamma}$ is the Kronecker delta and eq.(18) represent a set of K*K second order equations in the first order path derivatives. Together with eq.(13) a strategy for finding the solution can be formulated. This is explained in more detail in Section 2.4 for the case of a single load defined as a load path in load or displacement space.

At this stage, it is pertinent to comment on the first order perturbation problem derived here, as compared to the Riks(1979) arc length method. The Riks application was originally formulated in terms of only one load parameter, say Λ, and for the purpose of comparison, eq.(13) and eq.(18) will then be simplified to

$$f_i{}^j \dot{q}_j + f_i{}^\Lambda \dot{\Lambda} = 0 \qquad (19a)$$

$$\dot{q}_i \dot{q}_i + (\dot{\Lambda})^2 = 1 \qquad (19b)$$

A dot over the parameter symbolise the path derivative with respect to η, i.e. $\dot{q}_i \equiv \partial q_i / \partial \eta$, $\dot{\Lambda} \equiv \partial \Lambda / \partial \eta$ and $f_i{}^\Lambda \equiv \partial f_i / \partial \Lambda$ (η= s = arc length in Riks notation). Eq.(19) constitutes M linear equations and one second order equation in the unknowns $\dot{q}_i$ and $\dot{\Lambda}$, and are the same as given by Riks(1979). In the Riks method it is assumed that these first order rates have been computed and they are used as fixed numbers in the single load version of eq.(16), which can be written as

$$\Delta\eta = \dot{q}_i \Delta q_i + \dot{\Lambda}\Delta\Lambda \qquad (20)$$

In eq.(20) the following incremental parameters is introduced; $\Delta\eta = \eta - \eta_{,s}$, $\Delta q_i = (q_i - q_{i,s})$ and $\Delta\Lambda = (\Lambda - \Lambda_{,s})$. For a single load parameter the total equilibrium equations, eq.(1), are rewritten as

$$f_i(q_j + \Delta q_j, \Lambda + \Delta\Lambda) = 0 \qquad (21)$$

In the Riks method $\Delta\eta$ is specified as a small number. Assuming that eq.(20) is valid for this small value of $\Delta\eta$, eq.(20) together with eq.(21) is solved using a Newton-Raphson iteration procedure finding the incremental properties Δq_i and $\Delta\Lambda$. This is what is often referred to as the equilibrium control procedure.

By using eq.(20) an approximation is introduced in the Riks procedure valid for small values of the incremental arc length parameter $\Delta\eta$, and special techniques are applied in order to obtain valid solutions in the iterative procedure. This is not discussed further herein.

However, the present approach is to use the perturbation method in a straightforward incremental scheme. This means that the path derivatives will be used directly for finding the next equilibrium state and the use of eq.(20), eq.(21) and Newton-Raphson iterations on the total equilibrium equations are abonded.

The perturbation procedure is based on finding and using directly the path derivatives (rates) evaluated in a known state. For the present purpose an expansion to second order is explored, as this is consistent with the Koiter theory. Eq.(11) specialises for a single load parameter to

$$\begin{aligned} \Delta q_i &= \dot{q}_i \Delta\eta + \frac{1}{2!}\ddot{q}_i (\Delta\eta)^2 + \cdots \\ \Delta\Lambda &= \dot{\Lambda}\Delta\eta + \frac{1}{2!}\ddot{\Lambda}(\Delta\eta)^2 + \cdots \end{aligned} \tag{22}$$

Thus, knowing the path derivatives in a state, the next state can be found by specifying sufficiently small values of the arc length parameter $\Delta\eta$. Moreover, these path derivatives are exact in a known point and the approximation in the perturbation procedure is then related to the problem of how may terms in the expansion that needs to be included. In the present context only second order terms are used combined with sufficiently small values of the arc length parameter $\Delta\eta$. The second order term corresponds then, in a sense, to the equilibrium control in the Riks method.

The formulation of the second order problem is carried out in the following for a system of multiple loads.

Further by differentiation of eq.(13) once more gives with respect to some η_γ gives

$$\begin{aligned} &f_i{}^{jk} q_k{}^{\gamma} q_j{}^{\alpha} + f_i{}^{j} q_j{}^{\alpha\gamma} \\ &+ f_i{}^{\beta j} q_j{}^{\gamma} \Lambda_\beta{}^{\alpha} + f_i{}^{\beta\lambda} \Lambda_\lambda{}^{\gamma} \Lambda_\beta{}^{\alpha} + f_i{}^{\beta} \Lambda_\beta{}^{\alpha\gamma} = 0 \end{aligned} \qquad i = 1,2,...,M; \quad \alpha, \beta, \gamma, \lambda = 1,2,..., K \tag{23}$$

Similarly, by differentiation of eq.(18) once more gives with respect to some η_λ gives

$$q_i{}^{\alpha} q_i{}^{\gamma\lambda} + q_i{}^{\gamma} q_i{}^{\alpha\lambda} + \Lambda_\beta{}^{\alpha} \Lambda_\beta{}^{\gamma\lambda} + \Lambda_\beta{}^{\gamma} \Lambda_\beta{}^{\alpha\lambda} = 0 \tag{24}$$

Eq.(23) and eq.(24) constitutes a set of K*K*M+K*K*K linear equations in the same number of unknowns for finding the second order path derivatives. By utilising the symmetry properties of the second order path derivatives $q_i{}^{\gamma\lambda}$ and $\Lambda_\beta{}^{\gamma\lambda}$ in γ and λ, the number of unknowns and the corresponding equations will be reduced to (1/2)*(K^2+K)(M+K).

This sequence of differentiation can be carried out further to any order wanted. For practical purposes the necessity for higher order path derivatives is not obvious as the degree of expansion is strongly linked to the chosen increment size of the control parameter. In practical implementation, the increment size can be varied as function of degree of path complexity, that is as function of the curvature of the path. By applying a second order expansion approach, combined with some type of curvature dependent increment control, equilibrium paths can be followed. However, the general topic of selecting the optimum solution strategy will be strongly problem dependent and in the present report this is not discussed in any detail.

2.4 Loading sequences and definition of buckling

In buckling calculations the main objective is to identify the maximum values of the simultaneously acting physical loads Λ_1, Λ_2, Λ_3 .... etc. that the structure may carry. For multiply acting loads this means it is necessary to identify a *buckling (stability) boundary* (surface) in the load space. This *buckling boundary* can be described by an equation in the form

$$g_u = g_u(\Lambda_1, \Lambda_2, \Lambda_3 ....) = 0 \tag{25}$$

Loads outside this surface may be possible, but they will normally represent an advanced postbuckled or collapsed state that is of secondary importance in buckling assessments. Thus, it is of main importance to identify the buckling boundary $g_u = 0$ that represents the critical combination of loads at which the structure will collapse under the condition of load control, see Fig.3 and Fig.4.

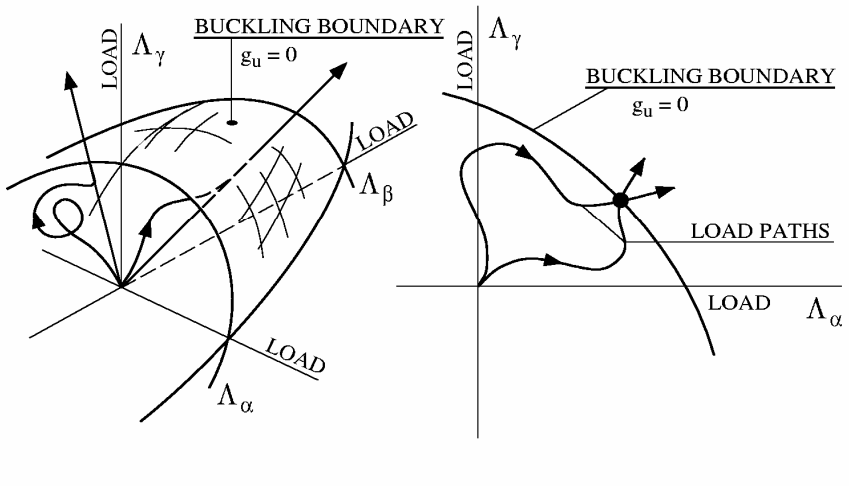

Fig. 4 Buckling boundary and load paths in load space

In practice, when a buckling calculation is to be carried out, it is necessary to relate the loads to each other in some way, i.e. to decide on the load path in load space, Fig.4. The definition of a load path in load space is done by specifying load functions in the form

$$\Lambda_\alpha = \Lambda_\alpha(t) \tag{26}$$

In eq.(26), t is the pseudo time parameter which is defined as taking positively increasing values along the load path and the load functions are always defined as single valued functions of t. This is a parametric representation of the load path in load space and the multiple load problem is transformed to a single parameter problem.

An automated calculation procedure will then determine at which point along the defined load path that corresponds to collapse/buckling of the structure. For combined loads this means

finding at which point the defined load path crosses the *buckling boundary* in load space as indicated in Fig.4. The present perturbation procedure identifies this cross point as the buckling point under load control. In the right most sketch in Fig.4 two different load paths is crossing at the same point on the buckling boundary. This illustrates that elastic material behaviour leads to a unique stability boundary independent of the load path.

The present perturbation procedure with arc length control is capable of tracing the equilibrium curve beyond the buckling point. In load space, immediate after the buckling boundary is reached, the equilibrium path will be traced in the direction of the tangent to the path at the buckling boundary, though in the reversed direction. The equilibrium path beyond the buckling boundary is called the postbuckling (or postcollapse) curve and represents descending loads close to the buckling boundary. The unloading may be sudden or more gradual depending on the structural problem analysed. This part of the equilibrium surface represent unstable equilibrium states in case of load control. However, in an advanced deflected state the loads may start to increase once more and even exceed the first stability boundary (e.g., as in case of snap-through of the classical shallow arc problem).
Thus, even though stable equilibrium states in some cases can be found outside the first buckling boundary, such states are associated with quite large displacements and they will normally have limited practical interest for design purposes.

For the case of a single load parameter Λ, it is possible to visualize the control parameter η as the arc length along the equilibrium curve in the Λ - q_i space, Fig.5a. Thus, we have a unique direction for a positive loading and the maximum possible value (locally) for Λ is identified as the load Λ_u corresponding to collapse under load control.

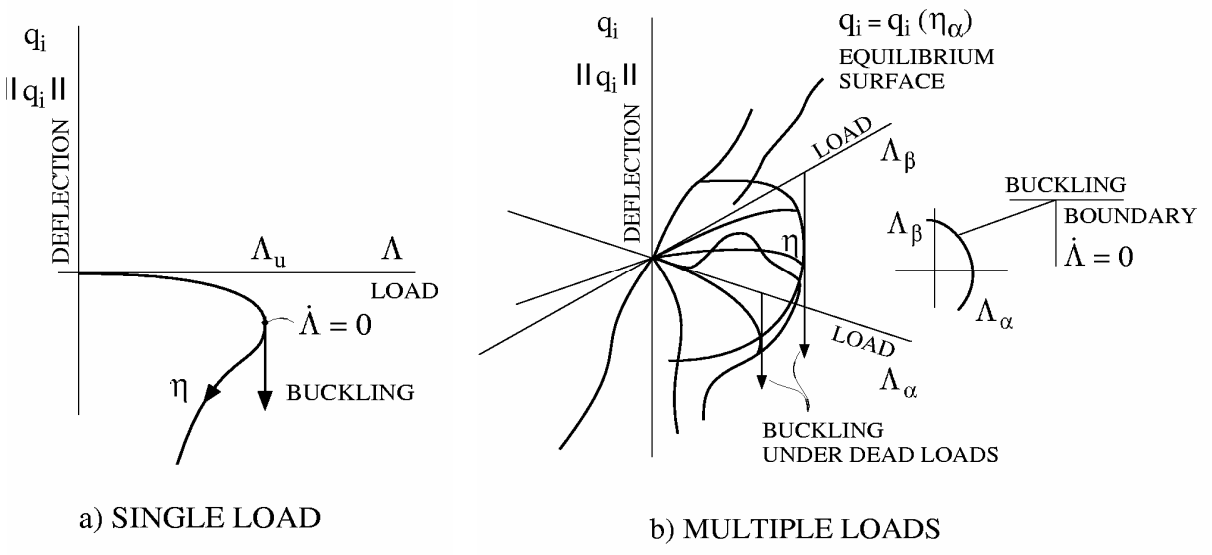

Fig.5 Equilibrium surfaces under multiple loads

For a set of multiple independent loads, the equilibrium surface will have folds and buckling under load control will take place for prescribed load paths that crosses these folds, Fig.5b or Fig.3. Viewed in the load space (Λ_α - Λ_β), the edges of the folded equilibrium surface will be

mapped as the *buckling boundary*. In the tension dominated regions no buckling boundary exists.

In order to reach the buckling boundary, the load path under multiple loads has to be specified. The most general case will be to prescribe a continuous, curved load path as given by eq.(26). In practise a continuous load path will be approximated by a set of subsequent linear loading segments. A point m in the load space is given the notation

$$(\Lambda_1, \Lambda_2, ..., \Lambda_K)_m \qquad m = 1,2,...,L \qquad (27)$$

By letting the number of linear piecewise load paths approach a high number ($L \Rightarrow \infty$) any continuous, arbitrary load path can be specified.

In an incremental perturbation scheme, each linear load path sequence can be traced by the use of a single load multiplier, Λ. This parameter is assigned values in the range 0-1 between any state m and m + 1, Fig.5. The index notation of I_m and I_{m+1} etc. should not be confused with the state indication of I_s, I_{s+1} etc. The m index is used for states along the piecewise linear prescribed load path, and I_s is any state on the equilibrium surface. In other words, along a prescribed load path in load space, there are many states I_s between state I_m and I_{m+1}. A state I_m may be defined outside the buckling boundary and it may be outside the equilibrium surface in general.

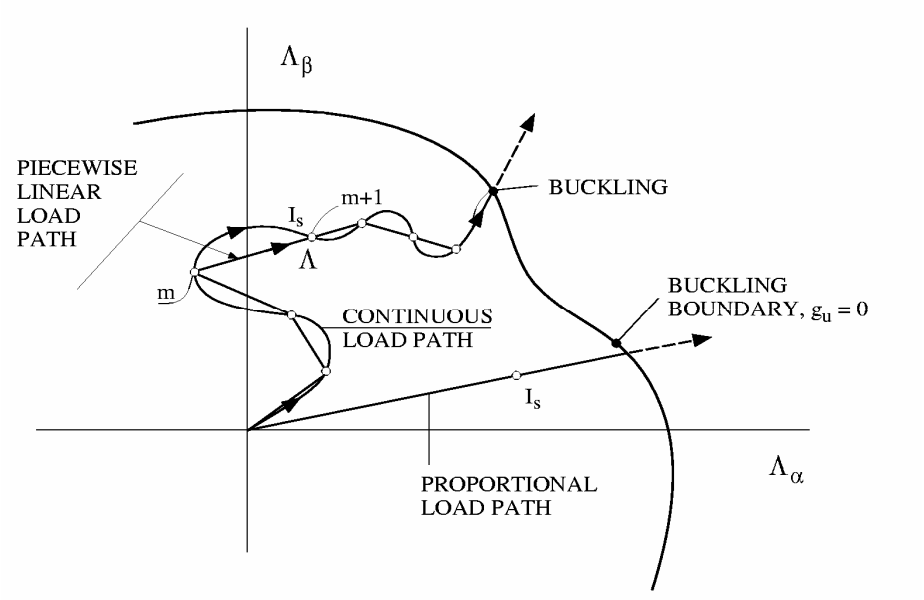

Fig.6 Piecewise linear loading sequence in load space

The definition of Λ as the single load multiplier during a general linear step in the specified load path follows from

$$\begin{aligned}
\Lambda_1 &= \Lambda_{1,m} + \Lambda(\Lambda_{1,m+1} - \Lambda_{1,m}) \\
\Lambda_2 &= \Lambda_{2,m} + \Lambda(\Lambda_{2,m+1} - \Lambda_{2,m}) \\
&\vdots \\
\Lambda_K &= \Lambda_{K,m} + \Lambda(\Lambda_{K,m+1} - \Lambda_{K,m})
\end{aligned} \tag{28}$$

Eq.(28) defines a piecewise proportional loading path through space, i.e. for $\Lambda = 0$ the loads correspond to state m, while by linearly scaling Λ to unity, state m+1 is reached. This procedure will be followed sequentially from the unloaded state to the final state defined.

With this definition of loading sequence under multiple loads, the equilibrium equations, eq.(1), can be written as

$$f_i(q_j, \Lambda_{\alpha,m} + \Lambda(\Lambda_{\alpha,m+1} - \Lambda_{\alpha,m})) = 0 \tag{29}$$

where Λ is the single load multiplier and $\Lambda_{\alpha,m}$ and $\Lambda_{\alpha,m+1}$ are considered to be fixed parameters for the actual loading segment to be traced. In each linear load sequence the solution may then be written as a function of a single parameter η as

$$\begin{aligned}
q_i &= q_i(\eta) \\
\Lambda &= \Lambda(\eta)
\end{aligned} \tag{30}$$

This solution expanded around I_s gives

$$\begin{aligned}
q_i &= q_{i,s} + \dot{q}_i(\eta - \eta_s) + \frac{1}{2!}\ddot{q}_i(\eta - \eta_s)^2 + \cdots \\
\Lambda &= \Lambda_s + \dot{\Lambda}(\eta - \eta_s) + \frac{1}{2!}\ddot{\Lambda}(\eta - \eta_s)^2 + \cdots
\end{aligned} \tag{31}$$

A single dot over the parameter symbolises the first order derivative with respect to η as explained before, two dots over the parameters symbolises second order derivative with respect to η etc.

In order to provide the sufficient number of equations, the perturbation parameter η has to be defined. As in Section 2.3 the arc length concept is adopted and eq.(16), is for the single load case, simplified to

$$\eta - \eta_s = \dot{q}_i(q_i - q_{i,s}) + \dot{\Lambda}(\Lambda - \Lambda_s) \tag{32}$$

Together with the equilibrium equations, i.e. eq.(29), this definition of the perturbation parameter gives a sufficient set of equations for a proper formulation of the problem. The unknowns in the problem are the path derivatives of the deflection parameters q_i, i.e.

$$\begin{matrix} \dot{q}_1, \dot{q}_2, \cdots, \dot{q}_M \\ \ddot{q}_1, \ddot{q}_2, \cdots, \ddot{q}_M \\ \vdots \end{matrix} \qquad (33)$$

and the path derivatives of the single load multiplier Λ, i.e.

$$\begin{matrix} \dot{\Lambda} \\ \ddot{\Lambda} \\ \vdots \end{matrix} \qquad (34)$$

The calculation of the change of each load component Λ_α along the load path follows from the expansion

$$\Lambda_\alpha = \Lambda_{\alpha,s} + \dot{\Lambda}_\alpha(\eta - \eta_s) + \frac{1}{2!}\ddot{\Lambda}_\alpha(\eta - \eta_s)^2 + \cdots \qquad (35)$$

The path derivatives of each load component follows from eq.(28), i.e.

$$\begin{matrix} \dot{\Lambda}_\alpha = \dot{\Lambda}(\Lambda_{\alpha,m+1} - \Lambda_{\alpha,m}) \\ \ddot{\Lambda}_\alpha = \ddot{\Lambda}(\Lambda_{\alpha,m+1} - \Lambda_{\alpha,m}) \\ \quad \vdots \end{matrix} \qquad (36)$$

Having provided the necessary non-linear algebraic equations, i.e. eq.(29) and eq.(32), the perturbation procedure will generate a sequence of equations which solved gives the path derivatives in state I_s. The following formulation is a specialisation of the multiple load parameter case presented in Section 2.3.

The first order partial differentiation of eq.(29) and eq.(32) with respect to η gives

$$f_i{}^j \dot{q}_j + f_i{}^\Lambda \dot{\Lambda} = 0 \qquad i,j = 1,\ldots,M \qquad (37a)$$

$$\dot{q}_i \dot{q}_i + \dot{\Lambda}^2 = 1 \qquad i,j = 1,\ldots,M \qquad (37b)$$

This gives M linear and one second order equation in the M+1 unknowns. They are the single load version of the multiple load equations as derived in Section 2.3 and as discussed in connection with the Riks method. Eq.(37b) is a second order equation and thus two solutions of the equations are possible. A strategy for selecting the relevant solution is needed and is explained in the following.

A column solution matrix for state I_s is assumed in the form

$$\dot{\mathbf{x}} = \begin{bmatrix} \dot{\Lambda} \\ \dot{q}_1 \\ \dot{q}_2 \\ \vdots \\ \dot{q}_M \end{bmatrix} \tag{38}$$

First, the linear set of equations in eq.(37) are rearranged to the following format

$$\begin{bmatrix} f_1^{\,1} & f_1^{\,2} & \cdots & f_1^{\,M} \\ f_2^{\,1} & f_2^{\,2} & \cdots & f_2^{\,M} \\ \vdots & \cdots & & \\ f_M^{\,1} & f_M^{\,2} & \cdots & f_M^{\,M} \end{bmatrix} \begin{bmatrix} \dot{q}_1 \\ \dot{q}_2 \\ \vdots \\ \dot{q}_M \end{bmatrix} = - \begin{bmatrix} f_1^{\,\Lambda} \\ f_2^{\,\Lambda} \\ \vdots \\ f_M^{\,\Lambda} \end{bmatrix} \dot{\Lambda} \tag{39}$$

or in the compact form as

$$\mathbf{f}\,\dot{\mathbf{q}} = -\mathbf{f}^{\Lambda}\dot{\Lambda} \tag{40}$$

where per definition

$$\mathbf{f} = \begin{bmatrix} f_1^{\,1} & f_1^{\,2} & \cdots & f_1^{\,M} \\ f_2^{\,1} & f_2^{\,2} & \cdots & f_2^{\,M} \\ \vdots & \cdots & & \\ f_M^{\,1} & f_M^{\,2} & \cdots & f_M^{\,M} \end{bmatrix} \quad \dot{\mathbf{q}} = \begin{bmatrix} \dot{q}_1 \\ \dot{q}_2 \\ \vdots \\ \dot{q}_M \end{bmatrix} \quad \mathbf{f}^{\Lambda} = \begin{bmatrix} f_1^{\,\Lambda} \\ f_2^{\,\Lambda} \\ \vdots \\ f_2^{\,\Lambda} \end{bmatrix} \tag{41}$$

The solution of eq.(41) with respect to $\dot{\mathbf{q}}$ is written as

$$\dot{\mathbf{q}} = \begin{bmatrix} d_1 \\ d_2 \\ \vdots \\ d_M \end{bmatrix} \dot{\Lambda} \tag{42}$$

where per definition

$$\begin{bmatrix} d_1 \\ d_2 \\ \vdots \\ d_M \end{bmatrix} \equiv -\mathbf{f}^{-1}\mathbf{f}^{\Lambda} \tag{43}$$

The solution of eq.(40) requires a non-singular matrix **f** , which is always satisfied except at critical points. In an incremental procedure the matrix **f** is never evaluated precisely at a critical point and thus the case of singular solutions is avoided. However, in order to have a complete numerical method, critical points should be identified as part of an automated procedure, but this topic is not pursued in this report.

By substituting eq.(42) into the second equation in eq.(37) two possible solutions for the $\dot{\mathbf{x}}$ are obtained. They are denoted by as

$$\dot{\mathbf{x}}_+ = \begin{bmatrix} 1 \\ d_1 \\ d_2 \\ \vdots \\ d_M \end{bmatrix} \dot{\Lambda}_+ \tag{44a}$$

and

$$\dot{\mathbf{x}}_- = \begin{bmatrix} 1 \\ d_1 \\ d_2 \\ \vdots \\ d_M \end{bmatrix} \dot{\Lambda}_- \tag{44b}$$

where

$$\dot{\Lambda}_\pm = \frac{1}{\pm\sqrt{1+(d_1{}^2 + d_2{}^2 + \cdots + d_M{}^2)}} \tag{44c}$$

The d_i constants are defined in eq.(43).

Obviously eq.(44) provides two solutions with the same numerical value but with opposite signs. In the M+1 dimensional space, spanned by the q_i and Λ, the different solutions will both correspond to unit tangent vectors along the equilibrium curve. One unit tangent will be in the direction of increasing arc length η and the other will be in the opposite direction. The solution of interest is corresponding to the continuos increase of the arc length as this describes the progress along the specified load path.

Which solution that corresponds to the continuous increase of the arc length parameter η, will depend on the actual state along the equilibrium path. Typically, the positive root is the correct in the origin (zero loads). The positive root will continue to be the correct until a point is reached where the first order rate of the load parameter becomes zero. This will be at the buckling point (singular point), or more specifically at the point where the load path intersects the buckling boundary. Beyond this point the negative root becomes the relevant choice, since

this describes progress along the equilibrium surface. In other words, when $\dot{\Lambda} = 0$ is found along the prescribed load path, the buckling point under combined loads are reached.

In an automated calculation procedure the correct solution needs to be picked up at each state evaluated. For this purpose a maximum smoothness philosophy can be used. The maximum smoothness of the equilibrium path can be expressed as the minimum angle between neighboring solution tangent vectors, say between the direction tangent vector in the previous known state I_{s-1} and the current I_s state. Mathematically a maximum smoothness criterion can be formulated as follows.

The first order solution, eq.(37), can be written as a tangent vector **t** to the equilibrium path in the solution space. It is defined as

$$\mathbf{t} = \dot{\Lambda}\mathbf{i}_\Lambda + \dot{q}_1\mathbf{i}_1 + \dot{q}_2\mathbf{i}_2 + \cdots + \dot{q}_M\mathbf{i}_M \tag{45}$$

The **i** are the unit vectors along the respective axes in solution space and **t** is, eq.(36b), the unit tangent vector. In order to provide a smooth equilibrium curve the angle between two successive tangent vectors, say between the state I_{s-1} and I_s should be small. This can be formulated by calculating the scalar product between the corresponding tangent vectors. The necessary condition for a smooth equilibrium path is that the scalar product is larger than zero. This corresponds to an angle between successive tangent vectors less than 90 degrees. This is expressed as

$$\dot{q}_{i,s-1}\dot{q}_{i,s} + \dot{\Lambda}_{s-1}\dot{\Lambda}_s > 0 \tag{46}$$

In eq.(46) summation is not carried out over s The small s as subscript is a state indicator only.

The criterion of eq.(46) is the same as formulated by Stoll(1994). The selection of the relevant solution is to decide whether

$$\dot{\Lambda}_+ > 0 \tag{47a}$$

or

$$\dot{\Lambda}_- < 0 \tag{47b}$$

Physically the positive solution corresponds to a state before buckling and the negative root corresponds to a state beyond buckling (i.e. after a local maxima/minima in Λ).

The perturbation procedure is very systematic and the expansion can be carried on to any order required. In an incremental perturbation scheme, the second order expansion is necessary as a compensation for the neglecting of equilibrium corrections. Second order expansion is the level used in the classical Koiter theory and it is considered to be an appropriate approximation as long as sufficiently small increments along the equilibrium curve is prescribed.

Differentiation of eq.(37) with respect to η gives

$$f_i^{\ jk}\dot{q}_k\dot{q}_j + 2f_i^{\ j\Lambda}\dot{q}_j\dot{\Lambda} + f_i^{\ j}\ddot{q}_j + f_i^{\ \Lambda\Lambda}\dot{\Lambda}^2 + f_i^{\ \Lambda}\ddot{\Lambda} = 0 \qquad (48a)$$

$$\dot{q}_i\ddot{q}_i + \dot{\Lambda}\ddot{\Lambda} = 0 \qquad (48b)$$

Eq.(48) are N+1 linear equations in N+1 unknowns for finding the second order path derivatives $\ddot{q}_j, \ddot{\Lambda}$.

With the path derivatives $\dot{q}_i, \ddot{q}_i \ldots, \dot{\Lambda}, \ddot{\Lambda}, \ldots$ known at state I_s, the new state I_{s+1} is found from eq.(31) by prescribing the incremental arc length parameter $\Delta\eta = (\eta - \eta_s)$ as a sufficiently small value.

2.5 Summary - incremental perturbation scheme

Chapter 2 gives a description of the perturbation method as a tool for solving non-linear structural problems with special emphasis on buckling strength assessment. The present application is within the solution of non-linear algebraic equations, which typically emerge, in structural theories formulated by using finite element or Rayleigh-Ritz discretizations of the displacement field. The most known application of the perturbation method is the theory developed by Koiter, Sewell, Thompson and others. In the literature the asymptotic Koiter theory has been used for detailed studies of postbuckling paths through critical points. However, the present approach is to apply the perturbation method in an incremental scheme. This means that the equilibrium curve of an imperfect structure is traced by stepping along the equilibrium path in small increments as is done in traditional incremental numerical schemes typically used in commercial finite element programs. By using the perturbation method up to a second order expansion around a known state, this can be an alternative to the traditional approach using Newton-Raphson iterations for equilibrium control.

For multiple acting loads it is shown how the perturbation procedure systematically provides parameters that describes the local shape of the equilibrium surface in all directions. These parameters are not used in the solution process directly, but are evaluated as a post-calculation feature at each known state with the purpose of estimating the current stiffness properties in all external load directions. The first order stiffness coefficients provided by the perturbation method is the same as the coefficients in the instaneous tangent stiffness matrix used in traditional finite element analyses. This application is more explored in Chapter 3.

In order to obtain solutions using the perturbation method, it is important to choose effective perturbation parameters. Section 2.2 describes the standard load or displacement control methods and the problems connected to their application are identified. In an automated incremental procedure the perturbation parameter has to be a continuously increasing variable along the specified load path. Obviously, for buckling problems applying a load control, the

load will not be a proper parameter, while a displacement parameter may serve the purpose. Thus, from a general point of view, an alternative to load or displacement control is needed and the direct arc length concept is adopted.

The direct arc length method is described for multiple loads in Section 2.3 and it is specialised for a single load parameter in Section 2.4. By choosing the arc length as perturbation parameter the problem of passing limit points have been solved. The present direct arc length method is discussed in relation to the arc length method first proposed by Riks(1979) within numerical analysis. It is identified that the first order perturbation solution is the same as the Riks method, but the application of the solution in the present perturbation scheme is different. The perturbation procedure proposed here applies the first order and second order solution directly in order to obtain the next equilibrium state while the Riks method applies the first order solution together with a Newton-Raphson equilibrium control using the total equilibrium equations.

The purpose of the present incremental perturbation procedure is to trace a load path across the equilibrium surface as schematically illustrated in Fig.2. The load path will in a practical case start in the origin of a rectangular coordinate system, which is normally defined to be an unloaded state. For the sake of overview it may be convenient to illustrate the incremental perturbation procedure in a flow chart as given in Fig.7. The starting point in a calculation loop is any known state I_s and the calculation procedure can briefly be summarised as follows.

1. A known equilibrium state is termed I_s and is located on the equilibrium surface. All state variables are treated as constants in a given state.

2. Calculate the first order and second order rates of change of the deflections and loads with respect to the chosen perturbation parameter, describing progress along the specified load path. These rates of change are found using sets of linear equations derived from the perturbation procedure. For convenience, the load-deflection curve can be viewed as a parametric space curve in a M+K dimensional rectangular coordinate system with the arc length along the curve as the independent perturbation parameter. The rates of change are calculated along this equilibrium curve. Applying the arc length concept, this means that the first order rate of change corresponds to the tangential direction of the load-deflection curve and the second order rate of change corresponds to the curvature. Higher order path derivatives beyond second order can be derived but are not considered in this report.

3. Calculate the first order and second order rates of change of the deflections and loads, which describes the shape of the equilibrium surface in different directions. These rates of change are found using sets of linear equations derived from the perturbation procedure and they can be used for assessing the current stiffness properties of the structure in the different load directions.

4. Calculate the new state I_{s+1} along the equilibrium curve, corresponding to the specified load path in load or displacement space, using the first order and second order rates of change of the deflections and loads as found in step 2. Possible limit points and snap buckling will be identified as cross-points between the specified load path and the buckling boundary.

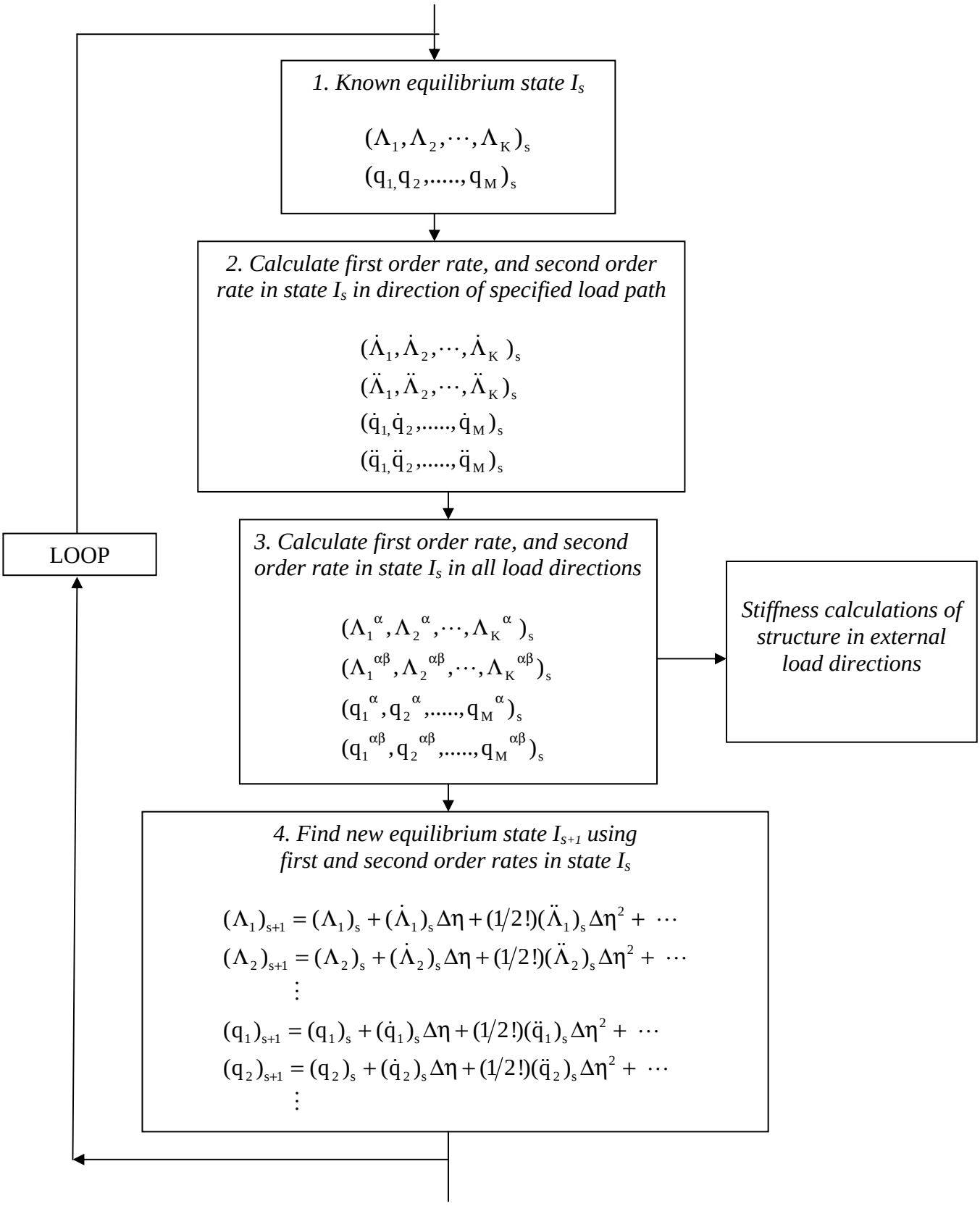

Fig. 7 Incremental perturbation scheme

3. STIFFNESS AND FLEXIBILITY PROPERTIES

3.1 General

In Chapter 2 the perturbation procedure was described as a general method for tracing equilibrium paths in the solution space spanned by M independent internal deflection parameters q_i and K independent external load parameters Λ_α or alternatively K external deflection parameters Δ_α. By specifying a load path in load space (Λ_1, Λ_2,…., Λ_K), or alternatively in deflection space (Δ_1, Δ_2,…. , Δ_K), the perturbation method was discussed in the context of tracing the equilibrium path in the M+K dimensional space with the localisation of the buckling boundary as the ultimate goal.

However, the stiffness properties of the structure have not been considered in an explicit manner so far and this item is explored in some detail in the present chapter. By stiffness properties are understood the change of an external load component per unit change of a corresponding external deflection component. In traditional linear analysis the stiffness matrix relates the external loads to the corresponding deflections. In non-linear analyses the tangent stiffness matrix relates the incremental loads to the corresponding incremental deflections.

In the following the stiffness evaluations is explored as a natural part of the incremental perturbation procedure and it is shown how the multiple path derivatives derived in Chapter 2 are used as parameters in the assessment of the stiffness coefficients. The stiffness estimates can be considered as a post-calculation feature using the multiple path derivatives already found as part of the solution process.

In this general introduction, stiffness coefficients up to second order are derived in order to illustrate the general principle. However, in Section 3.2 dealing with non-linear plate theory, only first order stiffness coefficients are derived as these represent the familiar tangent stiffness matrix and can be related to a clear physical understanding.

The most general way to describe the stiffness properties of a non-linear structure is to assume the existence of solutions relating the external loads to the corresponding prescribed external deflections, i.e.

$$\Lambda_\alpha = \Lambda_\alpha(\Delta_1, \Delta_2, ..., \Delta_K) \qquad \alpha = 1,2,...,K \qquad (49)$$

or alternatively, the inverse form expressing the deflections as functions of the external loads, i.e.

$$\Delta_\alpha = \Delta_\alpha(\Lambda_1, \Lambda_2, ..., \Lambda_K) \qquad \alpha = 1,2,...,K \qquad (50)$$

Such solutions are normally not possible to derive in closed form, but in an incremental perturbation procedure, the expanded form of these solutions can be utilised.

Eq.(49) gives the loads as function of deflections and is the natural form when a load path in the deflection space is defined. Eq.(50) gives the deflections as function of external loads and is the natural form when a load path in the load space is defined.

For illustration a case with displacement control is chosen. By expanding the load-deflection form of eq.(49) the stiffness properties appears as the coefficients in the series, i.e.

$$\Delta\Lambda_\alpha = K_{\alpha\beta}\Delta\Delta_\beta + K_{\alpha\beta\delta}\Delta\Delta_\beta\Delta\Delta_\delta + \cdots \qquad \alpha,\beta,\delta = 1, 2 ,..., K \qquad (51)$$

where per definition

$$K_{\alpha\beta} = \frac{\partial\Lambda_\alpha}{\partial\Delta_\beta}$$
$$K_{\alpha\beta\delta} = \frac{1}{2!}\frac{\partial^2\Lambda_\alpha}{\partial\Delta_\beta\partial\Lambda_\delta} \qquad \alpha,\beta,\delta = 1, 2 ,..., K \qquad (52)$$

The symbol Δ (without subscript) indicates incremental properties and eq.(51) gives a power series approximation around a known state I_s. $K_{\alpha\beta}$ is the first order stiffness coefficients which is the same as the tangent stiffness matrix in traditional finite element analysis. $K_{\alpha\beta\delta}$ is the second order stiffness coefficients representing the curvature of the load-deflection relation. The expansion can be carried out further, but at this stage the higher order stiffness coefficients are only of academic interest.

The basis for calculating the stiffness coefficients according to the definition of eq.(52) is to have compatibility conditions derived in an algebraic form, i.e. the external loads are expressed as functions of the external deflections and the internal degrees of freedom.

For the case of displacement control, the compatibility conditions will be non-linear functions in the form

$$\Lambda_\alpha = \Im_\alpha(\Delta_\beta, q_i) \qquad (53)$$

As an example, in Chapter 4 the functions $\Im_\alpha$ are derived for the case of biaxial loads of unstiffened plates.

In linear analysis eq.(53) resembles eq.(49) and the solution will take the linearized form

$$\Lambda_\alpha = K_{\alpha\beta}\Delta_\beta \qquad \alpha,\beta = 1, 2 ,..., K \qquad (54)$$

where $K_{\alpha\beta}$ are the elements in the linear stiffness matrix derived from the assumption of linear elastic material behaviour. For displacement control, solutions in the form of eq.(5) is substituted into eq.(53) to give

$$\Lambda_\alpha = \Im_\alpha(\Delta_\beta, q_i(\Delta_\beta)) \qquad (55)$$

By using eq.(52) and differentiating eq.(55) once with respect to any Δ_β it follows that

$$K_{\alpha\beta} = \frac{\partial \Im_\alpha}{\partial \Delta_\beta} + \frac{\partial \Im_\alpha}{\partial q_i}\frac{\partial q_i}{\partial \Delta_\beta} \qquad \alpha,\beta,\delta = 1, 2 ,..., K \qquad (56)$$

Similarly, using the definition of eq.(52) and differentiating eq.(56) with respect to any Δ_δ it follows that

$$K_{\alpha\beta\delta} = \frac{\partial^2 \Im_\alpha}{\partial \Delta_\beta \partial \Delta_\delta} + \frac{\partial^2 \Im_\alpha}{\partial \Delta_\beta \partial q_i}\frac{\partial q_i}{\partial \Delta_\delta} + \left(\frac{\partial^2 \Im_\alpha}{\partial q_i \partial \Delta_\delta} + \frac{\partial^2 \Im_\alpha}{\partial q_i \partial q_j}\frac{\partial q_j}{\partial \Delta_\delta}\right)\frac{\partial q_i}{\partial \Delta_\beta} + \frac{\partial \Im_\alpha}{\partial q_i}\frac{\partial^2 q_i}{\partial \Delta_\beta \partial \Delta_\delta} \qquad \alpha,\beta,\delta = 1, 2 ,..., K \qquad (57)$$

These derivations shows that the first order stiffness coefficients $K_{\alpha\beta}$ can be calculated for a known state I_s since they depend solely on the multiple path derivatives $\partial q_i / \partial \Delta_\beta$ calculated in case of displacement control, and the derivatives of the known compatibility functions $\Im_\alpha$.

Further, the second order stiffness coefficients depend on both the first order path derivatives $\partial q_i / \partial \Delta_\beta$ and second order path derivatives $\partial^2 q_i / \partial \Delta_\beta \partial \Delta_\delta$ and the derivatives of the known compatibility functions $\Im_\alpha$.

In the case of load control, the basis for the expansion will be eq.(50) and flexibility coefficients instead of stiffness coefficients are derived directly. The derivation of the flexibility coefficients will follow exactly the same procedure as described above, with eq.(53) inverted giving displacements as functions of loads as the basis, i.e.

$$\Delta_\alpha = \Re_\alpha(\Lambda_\beta, q_i) \qquad (58)$$

Since the expression for the flexibility coefficients are equivalent to the stiffness coefficients with the displacements Δ_α substituted for the loads Λ_α and vice a versa, these are not explicitly shown.

As discussed previously, neither direct application of load nor displacement control will be an effective strategy for solving buckling problems in general and the direct arc length method will be preferred. When applying the arc length method as the numerical method, the load or displacement control is to be understood solely as whether the specified load history is given in load or displacement space.

In order to avoid too much duplication, the illustration of this general case, is left to Section 3.4 where the stiffness properties of flat plate structures are described.

3.2 In-plane stiffness properties of flat plates

In analysing a structure of which a stiffened plate is the basic unit, it is of practical value to assess the in-plane stiffness of stiffened plate elements, which are subjected to combined in-plane loads and lateral pressure from sea or cargo. The purpose may be to illustrate the deviation from the normal assumption of linear elastic behavior described by Hooke's law, which are the basic prerequisite used in traditional FE analyses.

The instantaneous stiffness properties in the same directions as defined by the directions of the external loads are interesting from the point of view of structural redundancy and redistribution of forces. These stiffness (or flexibility) coefficients can be evaluated to any order, however, in this chapter the derivation is not shown further than to the first order. This corresponds to the familiar tangent stiffness properties in all load directions, which are properties that have a clear physical interpretation and which can be seen as representing the instantaneous linearized stiffness behaviour.

In Chapter 2 the multiple dimensional path derivatives, describing the local form of the equilibrium surface in all directions, were derived. These path derivatives are necessary parameters in the assessment of the stiffness coefficients as will be shown in this chapter. In order to be complete, both load control and displacement control are considered first as separate cases consistent with the treatment in Section 2.2. For the general case of load or displacement control of the load history in combination with arc length control for numerical solutions, the derivation of stiffness coefficients are shown in Section 3.4.4.

A stiffened plate is in principle a two dimensional structure in the x_1 - x_2 plane. The boundary of the plate lies in a flat plane and it is assumed that the plate edges remain straight during deformation. From an overall point of view the stiffened plate may be seen as an anisotropic macro material with general non-linear stress-strain relations. This means that the geometrically non-linear behaviour of the entire platefield is included in the macro material format. From a mathematical point of view this means that the internal degrees of freedom, q_i, are hidden in the macro format (i.e. hidden in the stiffness or flexibility coefficients), but of course they are present in the calculation of the equilibrium problem. Thus, the concept of a macro material is more a conceptual model rather than a physical one, as it may be attractive to see a locally buckled plate in a large structure as soft "material" as opposed to its unbuckled opponent.

In a material formulation it is natural to use the stress-strain symbols σ - ε , and the following notation is introduced

$$\begin{aligned}(\Lambda_1,\Lambda_2,...\Lambda_{K-1},\Lambda_K) &\equiv (\sigma_1,\sigma_2,...\sigma_{K-1},p)\\ (\Delta_1,\Delta_2,...\Delta_{K-1}) &\equiv (\varepsilon_1,\varepsilon_2,...,\varepsilon_{K-1})\end{aligned} \tag{59}$$

The σ_α are the in-plane average stresses (or loads per unit width) and the ε_β are the corresponding relative in-plane shortenings (average strains) of the plate edges. It is assumed that the plate edges is forced to remain in the plate plane during deformation (plate supported by a laterally stiff girder system or equivalent) and thus the out-of plane deflections of the plate edges are disregarded. The external displacement vector $(\varepsilon_1,\varepsilon_2,...,\varepsilon_{K-1})$ then only

represent the in-plane relative plate edge deflections. In the present notation the lateral pressure p is separated from the in-plane average stress σ_α due to the principal difference in response it produces.

For the present application of the in-plane load-shortening relations of flat plates, eq.(49) can be viewed as a generalisation of a non-linear material law, i.e. it is written in the present notation as

$$\sigma_\alpha = \sigma_\alpha(\varepsilon_1, \varepsilon_2, ...\varepsilon_{K-1}, p) \qquad \alpha = 1, 2, ..., (K-1) \qquad (60)$$

Eq.(60) can be seen as a non-linear material description of the plate response in which the internal degrees of freedom q_i are eliminated. More specifically this means that eq.(60) can be classified as a macro material description of the in-plane plate response in the sense that both the material law (i.e. Hooke's law) and the non-linear geometric behaviour of the entire platefield is included in the same formulation.

Eq.(60) is suited for strain control (strain = shortening = relative displacement of plate edges) since the loads are given as functions of the strains. The functional relationships of eq.(60) are not possible to derive in closed forms, but in an incremental perturbation procedure these total relations emerge in the expanded form around a known state I_s as

$$\begin{aligned}\Delta\sigma_\alpha &= C_{\alpha\beta}\Delta\varepsilon_\beta + C_{\alpha p}\Delta p \\ &+ C_{\alpha\beta\delta}\Delta\varepsilon_\beta\Delta\varepsilon_\delta + 2C_{\alpha\beta p}\Delta\varepsilon_\beta\Delta p + C_{\alpha pp}\Delta p^2 + \cdots\end{aligned} \qquad \alpha, \beta, \delta = 1, 2,., (K-1) \quad (61)$$

The macro material coefficients are defined by

$$\begin{aligned}C_{\alpha\beta} &\equiv \frac{\partial\sigma_\alpha}{\partial\varepsilon_\beta} \\ C_{\alpha p} &\equiv \frac{\partial\sigma_\alpha}{\partial p} \\ C_{\alpha pp} &\equiv \frac{1}{2!}\frac{\partial^2\sigma_\alpha}{\partial p^2} \\ C_{\alpha\beta\delta} &\equiv \frac{1}{2!}\frac{\partial^2\sigma_\alpha}{\partial\varepsilon_\beta\partial\varepsilon_\delta} \\ C_{\alpha\beta p} &\equiv \frac{1}{2!}\frac{\partial^2\sigma_\alpha}{\partial\varepsilon_\beta\partial p}\end{aligned} \qquad \alpha, \beta, \delta = 1, 2, ..., K\text{-}1 \qquad (62)$$

It is illustrative to use matrix notations and to retain only the first order terms. From eq.(61) the first order incremental relations between in-plane loads and in-plane displacements are written as

$$\begin{bmatrix} \Delta\sigma_1 \\ \Delta\sigma_2 \\ \vdots \\ \Delta\sigma_{K-1} \end{bmatrix} = \begin{bmatrix} C_{11} & C_{12} & \cdots & C_{1(K-1)} \\ C_{21} & C_{22} & \cdots & C_{2(K-1)} \\ \vdots & \vdots & \ddots & \vdots \\ C_{(K-1)1} & C_{(K-1)2} & \cdots & C_{(K-1)(K-1)} \end{bmatrix} \begin{bmatrix} \Delta\varepsilon_1 \\ \Delta\varepsilon_2 \\ \vdots \\ \Delta\varepsilon_{K-1} \end{bmatrix} + \begin{bmatrix} C_{1p} \\ C_{2p} \\ \vdots \\ C_{(K-1)p} \end{bmatrix} \Delta p \qquad (63)$$

C_{ij} is the tangent stiffness matrix and C_{ip} are the coefficients representing the change of in-plane loads per unit change of the lateral pressure. All coefficients are dependent on the state I_s at which they are evaluated.

For load control the inverted form of eq.(60) is more suited. This gives relations in the general form as

$$\varepsilon_\alpha = \varepsilon_\alpha(\sigma_1, \sigma_2, ...\sigma_{K-1}, p) \qquad \alpha = 1, 2, ..., K-1 \qquad (64)$$

and the shortenings can be calculated as functions of the specified loads. The expanded form of eq.(64) around a known state I_s are

$$\begin{aligned} \Delta\varepsilon_\alpha &= M_{\alpha\beta}\Delta\sigma_\beta + M_{\alpha p}\Delta p \\ &\quad + M_{\alpha\beta\delta}\Delta\sigma_\beta\Delta\sigma_\delta + 2M_{\alpha p\beta}\Delta\sigma_\beta\Delta p + M_{\alpha pp}\Delta p^2 + \cdots \end{aligned} \qquad \alpha,\beta = 1, 2, ..., (K-1) \qquad (65)$$

where the macro flexibility coefficients are defined by

$$\begin{aligned} M_{\alpha\beta} &\equiv \frac{\partial\varepsilon_\alpha}{\partial\sigma_\beta} \\ M_{\alpha p} &\equiv \frac{\partial\varepsilon_\alpha}{\partial p} \\ M_{\alpha pp} &\equiv \frac{1}{2!}\frac{\partial^2\varepsilon_\alpha}{\partial p^2} \qquad \alpha, \beta, \delta = 1, 2, ..., (K-1) \\ M_{\alpha\beta\delta} &\equiv \frac{1}{2!}\frac{\partial^2\varepsilon_\alpha}{\partial\sigma_\beta\partial\sigma_\delta} \\ M_{\alpha\beta p} &\equiv \frac{1}{2!}\frac{\partial^2\varepsilon_\alpha}{\partial\sigma_\beta\partial p} \end{aligned} \qquad (66)$$

It is illustrative to use matrix notations and to retain only the first order terms. From eq.(65) the first order incremental relations between strains and in-plane loads are written as

$$\begin{bmatrix} \Delta\varepsilon_1 \\ \Delta\varepsilon_2 \\ \vdots \\ \Delta\varepsilon_{K-1} \end{bmatrix} = \begin{bmatrix} M_{11} & M_{12} & \cdots & M_{1(K-1)} \\ M_{21} & M_{22} & \cdots & M_{2(K-1)} \\ \vdots & \vdots & \ddots & \vdots \\ M_{(K-1)1} & M_{(K-1)2} & \cdots & M_{(K-1)(K-1)} \end{bmatrix} \begin{bmatrix} \Delta\sigma_1 \\ \Delta\sigma_2 \\ \vdots \\ \Delta\sigma_{K-1} \end{bmatrix} + \begin{bmatrix} M_{1p} \\ M_{2p} \\ \vdots \\ M_{(K-1)p} \end{bmatrix} \Delta p \qquad (67)$$

M_{ij} is the tangent flexibility matrix and M_{ip} are the coefficients representing the change of in-plane shortenings per unit change of the lateral pressure. All coefficients are dependent on the state I_s at which they are evaluated.

The present introduction defines the in-plane stiffness and flexibility coefficients for flat plates. Section 3.4 illustrates how these coefficients are calculated using Marguerre's non-linear shallow plate theory.

3.3 Graphical description of stiffness properties

It may be useful to illustrate the in-plane stiffness relations or the flexibility relations graphically. The stiffness relations are given by eq.(60), i.e.

$$\sigma_\alpha = \sigma_\alpha(\varepsilon_1, \varepsilon_2, ...\varepsilon_{K-1}, p) \qquad \alpha = 1, 2, ..., (K-1) \qquad (68)$$

while the flexibility relations are the inverse, i.e.

$$\varepsilon_\alpha = \varepsilon_\alpha(\sigma_1, \sigma_2, ...\sigma_{K-1}, p) \qquad \alpha = 1, 2, ..., (K-1) \qquad (69)$$

Only the stiffness point of view is explained below since the flexibility version will be equivalent with shortenings, ε_α, taking the place of the loads, σ_α, and vice a versa.

From eq.(68) the (K-1) loads, σ_α, may be viewed as (K-1) multi-dimensional functions of the (K-1) independent shortening parameters ε_α and lateral pressure p. For fixed values of the loads σ_α, these functions will be mapped as potential curves in the deflection space, as illustrated in Fig.8. The gradient to the surface, eq.(68), is per definition

$$\nabla\sigma_\alpha = \frac{\partial\sigma_\alpha}{\partial\varepsilon_\beta}\mathbf{i}_\beta + \frac{\partial\sigma_\alpha}{\partial p}\mathbf{i}_p \equiv C_{\alpha\beta}\mathbf{i}_\beta + C_{\alpha p}\mathbf{i}_p \qquad (70)$$

and the gradient vector $\nabla\sigma_\alpha$ normal to the potential lines. In other words, the first order stiffness coefficients $C_{\alpha\beta}$ (and $C_{\alpha p}$) represent the components of the surface gradient of the macro material law. Included in the macro material law are both constitutive relations and geometrical non-linear effects of the whole platefield. In the present setting of in-plane stiffness evaluation, the maximum stiffness will follows from Hooke's law. Deviation from Hooke's law is due to initial out of flatness and buckling. Moreover, high stiffness will be associated with marginal buckling effects while low stiffness is associated with significant buckling effects.

If the orientation of the potential curves varies as a function on the loading, i.e. if they depend on the combination of acting loads, this indicates that buckling will influence the maximum/minimum stiffness directions. This is more discussed in the example included in Chapter 4 where also flexibility potential curves are included.

The load history is defined as a path in load or displacement space as discussed in Section 2.4. This path will be viewed as a curve starting at the origin and taking different directions according to the load path definition. Say, if the load history is defined in the load space as a straight line it will be mapped into the displacement space $(\varepsilon_1, \varepsilon_2, ..., \varepsilon_{K-1})$ as a curved path and vice a versa.

From the point of view of illustrating stiffness properties the load history is viewed in displacement space $(\varepsilon_1, \varepsilon_2, ..., \varepsilon_{K-1}, p)$. The load history may be directly specified in this space or calculated from a load history specification through solution of the equilibrium equations. In any case the equilibrium solution may be written as an equilibrium path in the load-shortening spaces (σ_1, ε_β, p), (σ_2, ε_β, p)... etc. as radius vectors $\mathbf{r}_1$, $\mathbf{r}_2$..., etc.

$$\mathbf{r}_\alpha(\eta) = \sigma_\alpha(\eta)\mathbf{i} + \varepsilon_\beta(\eta)\mathbf{i}_\beta + p(\eta)\mathbf{i}_p \qquad \alpha, \beta = 1,2...,K \qquad (71)$$

Here $\mathbf{i}$ is the unit vector in the direction of stress σ_α, $\mathbf{i}_\beta$ is the unit vector in the corresponding ε_β direction and $\mathbf{i}_p$ is the unit vector in the direction of lateral pressure p. If an equilibrium path is viewed in the displacement space $(\varepsilon_1, \varepsilon_2, ..., \varepsilon_{K-1}, p)$, it may take forms as illustrated in Fig.8. Fig. 8 illustrates two different equilibrium paths 1 and 2, which intersects at a given point. Through the same point is drawn a unique potential curve (σ_α = const.) with the gradient pointing in the direction of increasing load σ_α. By having only one potential curve through a given point it is illustrated that the strength and stiffness properties of structures, behaving according to the linear elastic material law, will not depend on the load history.

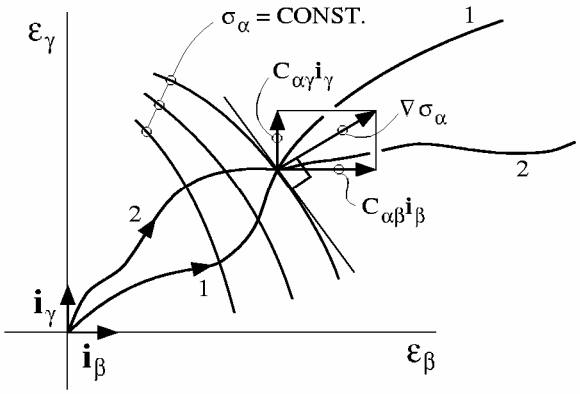

Fig.8. Geometrical interpretation of load-shortening stiffness

The tangent vector $\mathbf{t}_\alpha$ to the equilibrium path is the first derivatives of eq.(71).

$$\mathbf{t}_\alpha = \dot{\mathbf{r}}_\alpha(\eta) = \dot{\sigma}_\alpha(\eta)\mathbf{i} + \dot{\varepsilon}_\beta(\eta)\mathbf{i}_\beta + \dot{p}(\eta)\mathbf{i}_p \qquad (72)$$

which is a unit vector since η is the arc length along the curve. The curvature vector $\boldsymbol{\kappa}$ is defined as the second derivatives of the radius vector **r**, i.e. the curvature vector is given by the second derivatives of eq.(71).

$$\boldsymbol{\kappa}_\alpha = \ddot{\mathbf{r}}_\alpha(\eta) = \ddot{\sigma}_\alpha(\eta)\mathbf{i} + \ddot{\varepsilon}_\beta(\eta)\mathbf{i}_\beta + \ddot{p}(\eta)\,\mathbf{i}_p \tag{73}$$

The unit vector along the curvature vector is accordingly

$$\mathbf{n}_\alpha = \frac{\boldsymbol{\kappa}_\alpha}{\|\boldsymbol{\kappa}_\alpha\|} = \frac{\ddot{\sigma}_\alpha(\eta)}{\|\boldsymbol{\kappa}_\alpha\|}\mathbf{i} + \frac{\ddot{\varepsilon}_\beta(\eta)}{\|\boldsymbol{\kappa}_\alpha\|}\mathbf{i}_\beta + \frac{\ddot{p}(\eta)}{\|\boldsymbol{\kappa}_\alpha\|}\mathbf{i}_p \tag{74}$$

where

$$\|\kappa_\alpha\| = \left[(\ddot{\sigma}_\alpha)^2 + \ddot{\varepsilon}_\beta\ddot{\varepsilon}_\beta + (\ddot{p})^2\right]^{1/2} \tag{75}$$

The stiffness property in the direction of the load path is the scalar product of the surface gradient $\nabla\sigma_\alpha$ and the unit vector $\mathbf{t}_\varepsilon$ in the direction of the load path in the displacement space $(\varepsilon_1, \varepsilon_2, ..., \varepsilon_{K-1}, p)$, i.e.

$$C_\alpha \equiv \nabla\sigma_\alpha \cdot \mathbf{t}_\varepsilon \qquad \alpha = 1,2,..,(K\text{-}1) \tag{76}$$

The presented geometrical point of view may be useful for the understanding of the stiffness properties in general and the concept of potential curves may be illustrative for deciding the maximum/minimum directions of stiffness of the structure. Flexibility illustrations are the inverted point of view and both types of presentations are given in the example in Section 4.4.

3.4 Geometrically non-linear plate theory

3.4.1 General

For the purpose of buckling calculations, the von-Karman(1910) equations valid for moderate rotations have been used extensively in the literature. His theory is based on the classical Love-Kirchhoff hypothesis valid for thin shells. Marguerre(1938) extended the von-Karmans theory by adding initial out of flatness. This theory is frequently referred to as shallow shell theory (e.g. in Washizu(1975)) and is the basis for the equations given in the present chapter and Chapter 4. These theories are not described in any detail here as the reader may find a full account in e.g. Washizu(1975).

In Marguerre's non-linear plate theory the compatibility condition may be solved explicitly giving load-shortening-displacement relations in the general form (see eq.(53))

$$\sigma_\alpha = \Im_\alpha(\varepsilon_\beta, q_j) \tag{77}$$

In Chapter 4 the exact form of these equations are given for a single degree of freedom plate buckling model. These functions describe only compatibility between in-plane and out-of plane deflections excluding equilibrium. Eq.(77) is inverted to give

$$\varepsilon_\alpha = \Re_\alpha(\sigma_\beta, q_j) \tag{78}$$

When analysing a plate buckling problem the loading has to be specified as a path either in the load space (see Fig.6) or alternatively in the displacement space. Moreover, the most frequent method is to express equilibrium condition in terms of the loads. Typically will be the stationary condition of a potential energy V in which V is expressed in terms of a set of external prescribed loads σ_α . This leads to equilibrium equations in the form

$$f_i(\sigma_\alpha, q_i, p) = 0 \tag{79}$$

When a potential energy V in terms of loads is formulated, the applied external loads have been constrained to be independent. However, for stiffened panels that are parts of larger structures it may be more convenient to prescribe some external displacements rather than loads allowing then for load redistribution at the boundaries between different elements. Displacement control can also be formulated using the potential energy principle and leads to equations on the form

$$f_i(\varepsilon_\alpha, q_i, p) = 0 \tag{80}$$

Having specified the load path, the equilibrium states are found along this path, using the most appropriate solution procedure. The most simplified procedure will be to use the load or displacement control technique directly, as described in Section 3.4.2 and 3.4.3. However, as explained before, the more general procedure of direct arc length method is normally to be preferred and this procedure is described in Section 3.4.4.

The lateral pressure is per definition load intensity and is separated from the other load components. It can be combined with either the loads, σ_α, or displacements, ε_α, in the definition of the load history.

3.4.2 Displacement control

For direct displacement control of the solution, the basis is the equilibrium equations in the form of eq.(80). As illustrated in Section 2.2 solution to eq.(80) are sought in the form

$$q_j = q_j(\varepsilon_\beta, p) \tag{81}$$

Substituting eq.(81) into eq.(77) gives the macro material form

$$\sigma_\alpha = \Im_\alpha(\varepsilon_\beta, q_i(\varepsilon_\beta, p)) \tag{82}$$

Using the definition in eq.(62) together with the compatibility condition eq.(82), gives for the first order stiffness coefficients

$$C_{\alpha\beta} \equiv \frac{\partial \Im_\alpha}{\partial \varepsilon_\beta} + \frac{\partial \Im_\alpha}{\partial q_i}\frac{\partial q_i}{\partial \varepsilon_\beta} \tag{83a}$$

$$C_{\alpha p} \equiv \frac{\partial \Im_\alpha}{\partial p} + \frac{\partial \Im_\alpha}{\partial q_i}\frac{\partial q_i}{\partial p} \tag{83b}$$

The derivatives $\partial \Im_\alpha / \partial \varepsilon_\beta$, $\partial \Im_\alpha / \partial q_i$ are readily available from eq.(77). However, the path derivatives $\partial q_i / \partial \varepsilon_\alpha, \partial q_i / \partial p$ are found solving a linear set of equations. Substituting eq.(81) into eq.(80) gives the equilibrium equations in the form

$$f_i(q_j(\varepsilon_\beta, p), \varepsilon_\beta, p) = 0 \tag{84}$$

Differentiating eq.(84) once with respect to ε_β gives

$$\frac{\partial f_i}{\partial q_j}\frac{\partial q_j}{\partial \varepsilon_\beta} + \frac{\partial f_i}{\partial \varepsilon_\beta} = 0 \tag{85a}$$

$$\frac{\partial f_i}{\partial q_j}\frac{\partial q_j}{\partial p} + \frac{\partial f_i}{\partial p} = 0 \tag{85b}$$

which is a set of M*K linear equations for finding the path derivatives $\partial q_i / \partial \varepsilon_\beta, \partial q_i / \partial p$.

This shows that displacement control of the solution procedure gives direct calculation of the stiffness coefficients $C_{\alpha\beta}$ and $C_{\alpha p}$.

3.4.3 Load control

For direct load control of the solution, the basis is the equilibrium equations in the form of eq.(79). As illustrated in Section 2.2 solution to eq.(79) are sought in the form

$$q_j = q_j(\sigma_\beta, p) \tag{86}$$

Substituting eq.(86) into eq.(78) gives the inverted macro material form

$$\varepsilon_\alpha = \Re_\alpha(\sigma_\beta, q_i(\sigma_\beta, p)) \tag{87}$$

Using the definition in eq.(66) together with the compatibility condition eq.(87) gives for the first order flexibility coefficients

$$M_{\alpha\beta} \equiv \frac{\partial \Re_\alpha}{\partial \varepsilon_\beta} + \frac{\partial \Re_\alpha}{\partial q_i}\frac{\partial q_i}{\partial \varepsilon_\beta} \tag{88a}$$

$$M_{\alpha p} \equiv \frac{\partial \Re_\alpha}{\partial p} + \frac{\partial \Re_\alpha}{\partial q_i}\frac{\partial q_i}{\partial p} \tag{88b}$$

The derivatives $\partial \Re_\alpha / \partial \varepsilon_\beta$, $\partial \Re_\alpha / \partial q_i$ are readily available from eq.(78). However, the path derivatives $\partial q_i / \partial \sigma_\alpha$, $\partial q_i / \partial p$ are found solving a linear set of equations. Substituting eq.(86) into eq.(79) gives the equilibrium equations in the form

$$f_i(q_j(\sigma_\beta, p), \sigma_\beta, p) = 0 \tag{89}$$

Differentiating eq.(89) once with respect to σ_β gives

$$\frac{\partial f_i}{\partial q_j}\frac{\partial q_j}{\partial \sigma_\beta} + \frac{\partial f_i}{\partial \sigma_\beta} = 0 \tag{90a}$$

$$\frac{\partial f_i}{\partial q_j}\frac{\partial q_j}{\partial p} + \frac{\partial f_i}{\partial p} = 0 \tag{90b}$$

which is a set of M*K linear equations for finding the path derivatives $\partial q_i / \partial \sigma_\beta$, $\partial q_i / \partial p$.

This shows that load control of the solution procedure gives direct calculation of the flexibility coefficients $M_{\alpha\beta}$ and $M_{\alpha p}$.

3.4.4 Arc length method

As discussed in Section 2.1 the direct application of load or displacement control fails as solution strategies for cases associated with multiple valued equilibrium surfaces. However, in any case, a definition of a load path in the (σ_1 , σ_2 , … , p) space or in the displacement space (ε_1 , ε_2 , … , p) is needed. Thus, from this load history point of view, the case can be either load or displacement controlled. In order to obtain solutions for a general case the load or displacement control cases are combined with the application of the direct arc length method.

For illustration a load history, defined in the load space (σ_1 , σ_2 , … , p), is used below. According to the arc length procedure in Section 2.1 the solution of the equilibrium problem is sought in terms of a set of independent arc length parameters (η_1 , η_2 , … , η_{K-1}, p). In the present notation the solution in the form of eq.(10) is rewritten as

$$q_j = q_j(\eta_\beta, p) \tag{91a}$$

$$\sigma_\alpha = \sigma_\alpha(\eta_\beta, p) \tag{91b}$$

The first order expansion of eq.(91) reads

$$\Delta q_j = \frac{\partial q_j}{\partial \eta_\beta}\Delta\eta_\beta + \frac{\partial q_j}{\partial p}\Delta p \tag{92a}$$

$$\Delta \sigma_\alpha = \frac{\partial \sigma_\alpha}{\partial \eta_\beta}\Delta\eta_\beta + \frac{\partial \sigma_\alpha}{\partial p}\Delta p \tag{92b}$$

The path derivatives $q_i{}^\beta \equiv \partial q_i / \partial \eta_\beta$, $q_i{}^p \equiv \partial q_i / \partial p$, $\sigma_\alpha{}^\beta \equiv \partial \sigma_\alpha / \partial \eta_\beta$, $\sigma_\alpha{}^p \equiv \partial \sigma_\alpha / \partial p$ are found from the perturbation procedure for multiple loads as outlined in Section 2.2.

Substituting eq.(91a) into eq.(77) gives the macro material form

$$\sigma_\alpha = \Im_\alpha(\varepsilon_\beta, q_i(\eta_\beta, p)) \tag{93}$$

The first order in-plane stiffness coefficients are defined according to eq.(62). Using this definition in combination with eq.(93) gives

$$C_{\alpha\beta} \equiv \frac{\partial \Im_\alpha}{\partial \varepsilon_\beta} + \frac{\partial \Im_\alpha}{\partial q_i}\frac{\partial q_i}{\partial \eta_\gamma}\frac{\partial \eta_\gamma}{\partial \varepsilon_\beta} \tag{94a}$$

$$C_{\alpha p} \equiv \frac{\partial \Im_\alpha}{\partial p} + \frac{\partial \Im_\alpha}{\partial q_i}\frac{\partial q_i}{\partial \eta_\gamma}\frac{\partial \eta_\gamma}{\partial p} \tag{94b}$$

The derivatives $\partial \Im_\alpha / \partial \varepsilon_\beta$ and $\partial \Im_\alpha / \partial q_i$ ($\partial \Im_\alpha / \partial p = 0$) are readily available from eq.(77) by forming the partial derivatives of the known functions $\Im_\alpha$. The missing parameters are $\partial \eta_\gamma / \partial \varepsilon_\beta$ and $\partial \eta_\gamma / \partial p$. In order to provide these parameters eq.(78) is used. Substituting eq.(91) into eq.(78) gives

$$\varepsilon_\alpha = \Re_\alpha(\sigma_\beta(\eta_\gamma, p), q_i(\eta_\gamma, p)) \tag{95}$$

By differentiating eq.(95) with respect to any η_γ gives

$$\frac{\partial \varepsilon_\alpha}{\partial \eta_\gamma} = \frac{\partial \Re_\alpha}{\partial \sigma_\beta}\frac{\partial \sigma_\beta}{\partial \eta_\gamma} + \frac{\partial \Re_\alpha}{\partial q_i}\frac{\partial q_i}{\partial \eta_\gamma} \tag{96}$$

Similarly, by differentiating eq.(95) with respect to p gives

$$\frac{\partial \varepsilon_\alpha}{\partial p} = \frac{\partial \Re_\alpha}{\partial \sigma_\beta}\frac{\partial \sigma_\beta}{\partial p} + \frac{\partial \Re_\alpha}{\partial q_i}\frac{\partial q_i}{\partial p} \tag{97}$$

This provides equations for the direct calculation of the $\varepsilon_\alpha{}^\gamma \equiv \partial \varepsilon_\alpha / \partial \eta_\gamma$ and $p^\gamma \equiv \partial p / \partial \eta_\gamma$ coefficients. However, these coefficients are the inverted of the coefficients used for

calculating the stiffness parameters in eq.(94). The inverted coefficients are obtained by assuming the shortenings to depend on the arc length parameters as

$$\varepsilon_\alpha = \varepsilon_\alpha(\eta_\beta, p) \tag{98}$$

The first order expansion of eq.(98) gives in matrix notation

$$\Delta\varepsilon = \mathbf{J}\,\Delta\eta + \mathbf{J}^p\,\Delta p \tag{99}$$

where the Jacobian matrices are defined as

$$\mathbf{J} \equiv \begin{bmatrix} \frac{\partial\varepsilon_1}{\partial\eta_1} & \frac{\partial\varepsilon_1}{\partial\eta_2} & \cdots & \frac{\partial\varepsilon_1}{\partial\eta_{K-1}} \\ \frac{\partial\varepsilon_2}{\partial\eta_1} & \frac{\partial\varepsilon_2}{\partial\eta_2} & \cdots & \frac{\partial\varepsilon_2}{\partial\eta_{K-1}} \\ \vdots & \vdots & \ddots & \vdots \\ \frac{\partial\varepsilon_{K-1}}{\partial\eta_1} & \frac{\partial\varepsilon_{K-1}}{\partial\eta_2} & \cdots & \frac{\partial\eta_{K-1}}{\partial\eta_{K+1}} \end{bmatrix} = \left[\varepsilon_\alpha{}^\gamma\right] \tag{100a}$$

and

$$\mathbf{J}^p \equiv \begin{bmatrix} \frac{\partial\varepsilon_1}{\partial p} \\ \frac{\partial\varepsilon_1}{\partial p} \\ \vdots \\ \frac{\partial\varepsilon_{K-1}}{\partial p} \end{bmatrix} \tag{100b}$$

The symbol $\Delta\varepsilon$ is a column matrix notation for the K-1 edge shortenings, ε_α, and $\Delta\eta$ is a column matrix notation for the K-1 arc length parameters, η_α. Inverting eq. (99) gives

$$\Delta\eta = \mathbf{J}^{-1}\,\Delta\varepsilon - \mathbf{J}^{-1}\mathbf{J}^p\,\Delta p \tag{101}$$

where the inverted Jacobian matrices are defined as

$$\mathbf{J}^{-1} \equiv \begin{bmatrix} \frac{\partial\eta_1}{\partial\varepsilon_1} & \frac{\partial\eta_1}{\partial\varepsilon_2} & \cdots & \frac{\partial\eta_1}{\partial\,\varepsilon_{K-1}} \\ \frac{\partial\eta_2}{\partial\varepsilon_1} & \frac{\partial\eta_2}{\partial\varepsilon_2} & \cdots & \frac{\partial\eta_2}{\partial\,\varepsilon_{K-1}} \\ \vdots & \vdots & \ddots & \vdots \\ \frac{\partial\,p}{\partial\varepsilon_1} & \frac{\partial\,p}{\partial\varepsilon_2} & \cdots & \frac{\partial\,p}{\partial\varepsilon_{K-1}} \end{bmatrix} = \left[\eta_\gamma{}^\beta\right] \tag{102a}$$

$$\mathbf{J}^{-1}\mathbf{J}^{p} \equiv \begin{bmatrix} \dfrac{\partial \eta_1}{\partial p} \\ \dfrac{\partial \eta_1}{\partial p} \\ \vdots \\ \dfrac{\partial \eta_{K-1}}{\partial p} \end{bmatrix} \tag{102b}$$

These inverted Jacobians contain the final coefficients for evaluations of the stiffness parameters as defined in eq.(94).

For a prescribed load history in shortening space, the procedure for calculating in-plane stiffness properties follows exactly the same pattern as described above. The loads will take the place of shortenings and vice a versa. Thus, there is no need for a detailed presentation of this case.

3.5 Summary

The present chapter starts with a general description of the non-linear stiffness properties of structures. The expanded form of the non-linear load-deflection relations defines the current stiffness coefficients. Moreover, by providing compatibility conditions in a special functional form, the connection between the stiffness coefficients and the path derivatives available from the perturbation procedure is established.

The stiffness properties are discussed in more detail in connection with in-plane behaviour of flat plates. The geometrical point of view of potential lines are described as a way of illustrating the continuous change of stiffness (or flexibility) of plates as a function of the applied loading. For the purpose of having a simple notation, the concept of macro material is introduced embracing both the constitutive and geometrically non-linear behaviour of the whole panel into one pseudo material model.

The procedure for calculating stiffness properties of flat plates within Marguerre’s plate theory is discussed. The general case of a direct arc length method and the connection to the path derivatives for multiple loads is given a detailed treatment. As special cases are included the more simplified load and displacement control cases.

4. APPLICATION ON A BIAXIALLY LOADED RECTANGULAR UNSTIFFENED PLATE

4.1 General

As an example the case of a rectangular plate subjected to biaxial compression has been analysed. The main purpose is to illustrate the macro material properties in the form of stiffness and flexibility coefficients. Secondly, the incremental perturbation procedure as a numerical tool has been tested even though it is realised that the example is very simplified as it involves only a single degree of freedom. The advantage of using a single degree of freedom model is that a closed form solution exist and comparisons with numerical results is then gives some measurements of the efficiency of the procedures. A more extensive three degree of freedom model handling mode interactions in stiffened panels is treated in Steen(1999).

The other purpose of the present example is to demonstrate how the in-plane stiffness (and flexibility) properties change for plates subjected to biaxial loads. Particularly, the region of compressive stresses will influence the stiffness properties and is of special interest.

Within the assumptions of Marguerre's plate theory Steen (1984) showed that the potential energy of an isotropic simply supported unstiffened rectangular plate subjected to biaxial loads and lateral pressure has the form

$$V = \frac{\pi^4}{256} E(2q_1 q_{10} + q_1^{\,2})^2 (k_1^{\,2} + k_2^{\,2}) + \frac{\pi^4}{96(1-\nu^2)} E q_1^{\,2} (k_1 + k_2)^2 - \frac{\pi^2}{8}(2q_1 q_{10} + q_1^{\,2})(k_1\sigma_1 + k_2\sigma_2) - \frac{4}{\pi^2} p q_1 \tag{103}$$

where per definition

$$q_1 = \frac{w}{t_p}, \quad q_{10} = \frac{\delta}{t_p}$$
$$k_1 = \left(\frac{t}{\ell_1}\right)^2 \quad , \tag{104}$$
$$k_2 = \left(\frac{t}{\ell_2}\right)^2 \quad ,$$

The potential energy V, eq.(103), is expressed in terms of the load σ_1 in the longitudinal direction (x_1-direction), the load σ_2 in transverse direction (x_2-direction) and lateral pressure p normal to the plate plane (x_3-direction) and this form is appropriate for load control of the load history. Furthermore, q_1 is the additional deflection amplitude normal to the plate plane, which is to be associated with a chosen buckling half length ℓ_1 in the x_1-direction and ℓ_2 in the x_2-direction, and q_{10} is the corresponding initial imperfection amplitude taken to be in the

same form. In the present application the half wavelengths are considered as having fixed values. These half wavelengths can be found from e.g. an eigenvalue minimisation procedure when the load history is defined. The assumption of a fixed buckling shape pattern limits the range of validity of the present model, since mode change during the load history is not captured. An example, demonstrating the effect of this limitation, is presented in Section 4.4.

The deflection parameters q_1 and q_{10} are non-dimensional versions of the lateral deflection amplitude w and δ, respectively. The scaling parameter has been chosen as the plate thickness t_p, see eq.(104). In eq.(103), E and ν are the isotropic material parameters, i.e. Young's modulus and Poisson's ratio respectively.

It was further shown (Steen 1984) that the load-shortening-deflection relations in the general total form (i.e. eq.(77); $\Im_\alpha$ functions) can be written as

$$\begin{aligned}\sigma_1 &= \frac{E}{1-\nu^2}(\varepsilon_1+\nu\varepsilon_2) - \frac{\pi^2}{8}\frac{E}{1-\nu^2}({q_1}^2+2q_{10}q_1)(k_1+\nu k_2)\\ \sigma_2 &= \frac{E}{1-\nu^2}(\varepsilon_2+\nu\varepsilon_1) - \frac{\pi^2}{8}\frac{E}{1-\nu^2}({q_1}^2+2q_{10}q_1)(k_2+\nu k_1)\end{aligned} \tag{105}$$

which inverted gives (eq.(78); $\Re_\alpha$ functions)

$$\begin{aligned}\varepsilon_1 &= \frac{1}{E}(\sigma_1-\nu\sigma_2) + \frac{\pi^2}{8}({q_1}^2+2q_{10}q_1)k_1\\ \varepsilon_2 &= \frac{1}{E}(\sigma_2-\nu\sigma_1) + \frac{\pi^2}{8}({q_1}^2+2q_{10}q_1)k_2\end{aligned} \tag{106}$$

Equilibrium equations in the form of eq.(79) can be derived from the principle of stationary potential energy, i.e.

$$f_1(q_1,\sigma_\alpha,p) \equiv \frac{\partial V}{\partial q_1} = 0 \qquad \alpha = 1,2 \tag{107}$$

From the definition of eq.(107) and eq.(103) it follows that the equilibrium equation is

$$\begin{aligned}f_1 \equiv{}& \frac{\pi^4}{64}E(2q_1q_{10}+{q_1}^2)(q_1+q_{10})({k_1}^2+{k_2}^2) + \frac{\pi^4}{48(1-\nu^2)}Eq_1(k_1+k_2)^2\\ &-\frac{\pi^2}{4}(q_{10}+q_1)(k_1\sigma_1+k_2\sigma_2) - \frac{4}{\pi^2}p = 0\end{aligned} \tag{108}$$

4.2 Numerical solution – Perturbation scheme

4.2.1 General

In the following the necessary equations are given for solving the equilibrium problem of a biaxially loaded plate under the condition of a prescribed path in the load space. These equations can be used for any prescribed path in general, but herein they are used for the purpose of illustration stiffness properties of plates. This means that the load paths are given a special form in load space in order to provide the sought stiffness contour plots as explained in more detail in Section 4.2.2. Alternatively, a set of equations can be derived appropriate for displacement control and for the purpose of illustrating flexibility curves. Both approaches are used in order to generate the results in Section 4.4.

The definition of a single load parameter Λ, describing any multi-linear load path through load space, is according to eq.(28)

$$\begin{aligned} \sigma_1 &= \sigma_{1,m} + \Lambda(\sigma_{1,m+1} - \sigma_{1,m}) \\ \sigma_2 &= \sigma_{2,m} + \Lambda(\sigma_{2,m+1} - \sigma_{2,m}) \\ p &= p_m + \Lambda(p_{m+1} - p_m) \end{aligned} \tag{109}$$

Eq.(109) is substituted into eq.(108), and the equilibrium equations thus shift from one set to the next, depending on which linear piece of the load path that is currently traced.

The assumed perturbation solution along the prescribed load path, expanded around a state I_s , is

$$\begin{aligned} \Delta q_i &= q_i \Delta\eta + \frac{1}{2!}\ddot{q}_i(\Delta\eta)^2 + \cdots \\ \Delta\Lambda &= \dot{\Lambda}\Delta\eta + \frac{1}{2!}\ddot{\Lambda}(\Delta\eta)^2 + \cdots \end{aligned} \tag{110}$$

The first order path derivatives of the loads are

$$\begin{aligned} \dot{\sigma}_1 &= \dot{\Lambda}(\sigma_{1,m+1} - \sigma_{1,m}) \\ \dot{\sigma}_2 &= \dot{\Lambda}(\sigma_{2,m+1} - \sigma_{2,m}) \\ \dot{p} &= \dot{\Lambda}(p_{m+1} - p_m) \end{aligned} \tag{111}$$

and second order path derivatives

$$\begin{aligned} \ddot{\sigma}_1 &= \ddot{\Lambda}(\sigma_{1,m+1} - \sigma_{1,m}) \\ \ddot{\sigma}_2 &= \ddot{\Lambda}(\sigma_{2,m+1} - \sigma_{2,m}) \\ \ddot{p} &= \ddot{\Lambda}(p_{m+1} - p_m) \end{aligned} \tag{112}$$

The loads along the equilibrium path are calculated from

$$\begin{aligned}\Delta\sigma_1 &= \dot{\sigma}_1\Delta\eta + \frac{1}{2!}\ddot{\sigma}_1(\Delta\eta)^2 + \cdots \\ \Delta\sigma_1 &= \dot{\sigma}_1\Delta\eta + \frac{1}{2!}\ddot{\sigma}_1(\Delta\eta)^2 + \cdots \\ \Delta p &= \dot{p}\Delta\eta + \frac{1}{2!}\ddot{p}(\Delta\eta)^2 + \cdots\end{aligned} \tag{113}$$

Knowing the loads, the end-shortenings may be calculated from the total relations, eq.(106).

Applying the direct arc length method for tracing the equilibrium path, the first and second order sets of perturbation equations for the single degree of freedom plate buckling model is given below.

The first order perturbation equations are taken from eq.(37), i.e. the first order solution is found by solving the following set of equations

$$\begin{aligned}f_1^{\,1}\dot{q}_1 + f_1^{\,1}\dot{\Lambda} &= 0 \\ \dot{q}_1\dot{q}_1 + \dot{\Lambda}^2 &= 1\end{aligned} \tag{114}$$

The coefficients in the first order equations are

$$\begin{aligned}f_1^{\,1} &= \frac{\pi^4}{64}E(3q_1^{\,2} + 6q_1q_{10} + 2q_{10}^{\,3})(k_1^{\,2} + k_2^{\,2}) + \frac{\pi^4}{48(1-\nu^2)}E(k_1 + k_2)^2 \\ &- \frac{\pi^2}{4}q_{10}(k_1\sigma_1 + k_2\sigma_2) \\ f_1^{\,\Lambda} &= -\frac{\pi^2}{4}q_{10}(k_1(\sigma_{1,m+1} - \sigma_{1,m}) + k_2(\sigma_{2,m+1} - \sigma_{2,m})) - \frac{4}{\pi^2}(p_{m+1} - p_m)\end{aligned} \tag{115}$$

The second order solution is found from eq.(48), i.e.

$$\begin{aligned}f_1^{\,11}\dot{q}_1\dot{q}_1 + 2f_1^{\,1\Lambda}\dot{q}_1\dot{\Lambda} + f_1^{\,1}\ddot{q}_1 + f_1^{\,\Lambda}\ddot{\Lambda} &= 0 \\ \dot{q}_1\ddot{q}_1 + \dot{\Lambda}\ddot{\Lambda} &= 0\end{aligned} \tag{116}$$

The coefficients in the second order equations are

$$\begin{aligned}f_1^{\,11} &= \frac{3\pi^4}{32}E(q_1 + q_{10})(k_1^{\,2} + k_2^{\,2}) \\ f_1^{\,1\Lambda} &= 0\end{aligned} \tag{117}$$

Following the scheme as summarised in Section 2.5 any specified path in load space can be traced.

4.2.2 Flexibility and stiffness calculation

For the purpose of illustrating the flexibility or stiffness properties of plates, potential curves as generally described in Section 3.3, may be used as an alternative to the conventional load-shortening presentation. It has the advantage of embracing a lot of information of the plate's strength in different directions into one diagram and it is a form that is consistent with the macro material concept. The terminology of contour plot is also commonly used for illustrating variations of two-dimensional functions and this notation is used herein with the same meaning as potential curves.

In Section 4.2.1 the equilibrium equation was derived in terms of loads and not displacements. It follows then that stiffness curves may be generated by prescribing a set of load histories in load space, (σ_1 - σ_2) according to the pattern described below. By mapping the corresponding response curves in the shortening space (ε_1 - ε_2), contour lines emerge illustrating the stiffness properties.

Since a stiffness curve is valid for a fixed value of a load parameter, say σ_1= 0,6 σ_F (σ_F is the yield stress of the material), the load history has to be prescribed in two steps. The first step will be to increase the load acting in one direction, say σ_1, up to the desired level. This level of σ_1 can be reached by prescribing any general load path in load space. A natural choice will be to define a linear path by scaling up the load σ_1 to the actual desired value, while simultaneously prescribing σ_2 to be zero. The next step will then be to fix the σ_1 value while prescribing an increased or decreased value of the other load parameter σ_2. By mapping the response in the shortening space, ε_1 - ε_2, and by retaining only the second sequence, the potential stiffness curve will be visualised as a curve valid for a fixed value of, say σ_1. By generating a set of potential curves with the same incremental load value, $\Delta\sigma_1$= fixed, between each curve, a map is generated that illustrates the stiffness for load direction σ_1.

The procedure described above gives potential curves for stiffness evaluations of the plate in an overall sense. It is a way of describing the plate's ability to carry loads in the different loading directions, and it has to be seen as an alternative method for strength and stiffness presentation. Moreover, to generate these curves requires many load histories to be calculated.

The normal case for strength evaluation will be to have a given load history and to estimate the strength following this prescribed load path. The present method, using the arc length approach, provides the calculation of the stiffness coefficients C_{11}, C_{12} and C_{22} along the specified path using the procedure as outlined Section 3.4.4.

For the purpose of practical applications it is useful with closed form solutions. In Section 4.3 the present single mode analysis is rewritten in a compact closed form and the stiffness coefficients are given explicitly. In Section 4.4, contour plots for both flexibility and stiffness properties are presented for a square plate and comparisons between closed form solution, perturbation solution and numerical results using ABAQUS are presented.

4.3 Closed form solution

Eq.(108) is the equilibrium equation for the case of biaxial loading and lateral pressure. By defining a parameter Λ_σ as

$$\Lambda_\sigma = \frac{12(1-\nu^2)}{\pi^2 E}\left(\frac{\ell_2}{t}\right)^2 \frac{((\ell_2/\ell_1)^2\sigma_1 + \sigma_2)}{(1+(\ell_2/\ell_1)^2)^2} \tag{118}$$

and neglecting the lateral pressure, p, eq.(108) may be rewritten in the following compact form

$$\Lambda_\sigma = \frac{q_1}{q_1+q_{10}}(1 + a_2(q_1^{\,2} + 3q_1q_{10} + 2q_{10}^{\,2})) \tag{119}$$

where per definition

$$a_2 = \frac{3}{4}(1-\nu^2)\frac{1+(\ell_2/\ell_1)^4}{(1+(\ell_2/\ell_1)^2)^2} \tag{120}$$

The parameter Λ_σ is a load parameter, representing the combined load effect. It takes the value of unity at the classical buckling level for combined loads (eigenvalues).

By substituting eq.(106) into eq.(119), with the purpose of eliminating the loads at the expense of the shortenings, and now defining a parameter Λ_ε as

$$\Lambda_\varepsilon = \frac{12}{\pi^2}\left(\frac{b}{t}\right)^2 \frac{((\ell_2/\ell_1)^2+\nu)\varepsilon_1 + (\nu(\ell_2/\ell_1)^2+1)\varepsilon_2}{(1+(\ell_2/\ell_1)^2)^2} \tag{121}$$

the following closed form equilibrium equation is found

$$\Lambda_\varepsilon = \frac{q_1}{q_1+q_{10}}(1 + b_2(q_1^{\,2} + 3q_1q_{10} + 2q_{10}^{\,2})) \tag{122}$$

where per definition

$$b_2 = \frac{3(3-\nu^2)(1+(\ell_2/\ell_1)^4) + 12\nu(\ell_2/\ell_1)^2}{4(1+(\ell_2/\ell_1)^2)^2} \tag{123}$$

For comparison, the Koiter theory (Hutchinson and Koiter 1970) gives the following form of the equilibrium equation

$$\Lambda_\sigma = \frac{q_1}{q_1 + q_{10}}(1 + a_2 {q_1}^2) \tag{124}$$

It is seen that the present closed form solution for plates, based on Marguerre's plate theory, is very similar to the Koiter equation apart from two terms coupled to the initial imperfection amplitude q_{10}. For small imperfection amplitudes the two solutions converge while for larger imperfection amplitudes the present solution predicts more optimistic results.

The in-plane stiffness properties, expressed by the $C_{\alpha\beta}$, will be load dependent and the coefficients at each load level can be calculated using the perturbation procedure as described in Section 3.4. However, it is possible to derive analytical expressions for the stiffness coefficients in the case of zero load and valid for a geometrically imperfect plate. Using the method in Section 3.4 and after a lot of tedious algebra, the following expressions emerge

$$\begin{aligned}
C_{11} &= \frac{E}{1-\nu^2}\left[1 - 6\frac{(k_1 + \nu k_2)^2}{A}\right] \\
C_{12} &= \frac{E\nu}{1-\nu^2}\left[1 - \frac{6}{\nu}\frac{(k_1 + \nu k_2)(k_2 + \nu k_1)}{A}\right] = C_{21} \\
C_{22} &= \frac{E}{1-\nu^2}\left[1 - 6\frac{(k_2 + \nu k_1)^2}{A}\right]
\end{aligned} \tag{125}$$

where per definition

$$A \equiv \frac{2(k_1 + k_2)^2}{{q_{10}}^2} + 3(3 - \nu^2)({k_1}^2 + {k_2}^2) + 12\nu k_1 k_2 \tag{126}$$

The same method can be used for derivation of the stiffness coefficients of a geometrically perfect plate ($q_{10} = 0$). In that case these coefficients are often referred to as the initial postbuckling coefficients as they describe the stiffness at the point of initial buckling following the deformations into the subsequent postbuckling region. The stiffness coefficients are expressed as in eq.(125) but with the coefficient A calculated from

$$A \equiv 3(3 - \nu^2)({k_1}^2 + {k_2}^2) + 12\nu k_1 k_2 \tag{127}$$

instead of from eq.(126). Comparing eq.(126) and eq.(127) shows that the initial postbuckling stiffness properties of geometrically perfect plates are constants and equal to the initial stiffness of plates with large initial imperfections ($q_{10} >> 1$).

For a perfect square plate the postbuckling stiffness coefficients defined by eq.(125) and eq.(127) takes the compact form

$$C_{11} = \frac{E^*}{1-(\nu^*)^2}$$
$$C_{12} = \frac{E^*\nu^*}{1-(\nu^*)^2} = C_{21} \qquad (128)$$
$$C_{22} = \frac{E^*}{1-(\nu^*)^2}$$

Here the modified material constants E* and ν^* are defined as

$$E^* = \frac{1}{2}E$$
$$\nu^* = -\frac{1}{2}(1-\nu) \qquad (129)$$

From these simple expressions it is concluded that an elastically buckled square plate has stiffness properties as an elastic isotropic material with 50% of Young's modulus and with a negative Poisson effect equal to -0.35 for steel material with $\nu = 0.3$.

4.4 Numerical results - Comparative study

For comparison purposes between the closed form solution and the numerical perturbation procedure a square plate with the following properties have been analyzed

$$\left.\begin{array}{l} a = 1000 \ \text{mm} \\ b = 1000 \ \text{mm} \\ t = 12 \ \text{mm} \end{array}\right\} \frac{b}{t} = 83 \qquad \begin{array}{l} E = 210\,000 \ \text{MPa} \\ \nu = 0.3 \\ (\sigma_F = 355 \ \text{MPa}) \end{array} \qquad (130)$$

However, before presenting the non-linear results for the plate, it is of interest to first illustrate contour plots according to Hooke's law for a material micro point. Flexibility curves for in-plane strain ε_1 for a biaxial stress situation are shown in Fig.9.

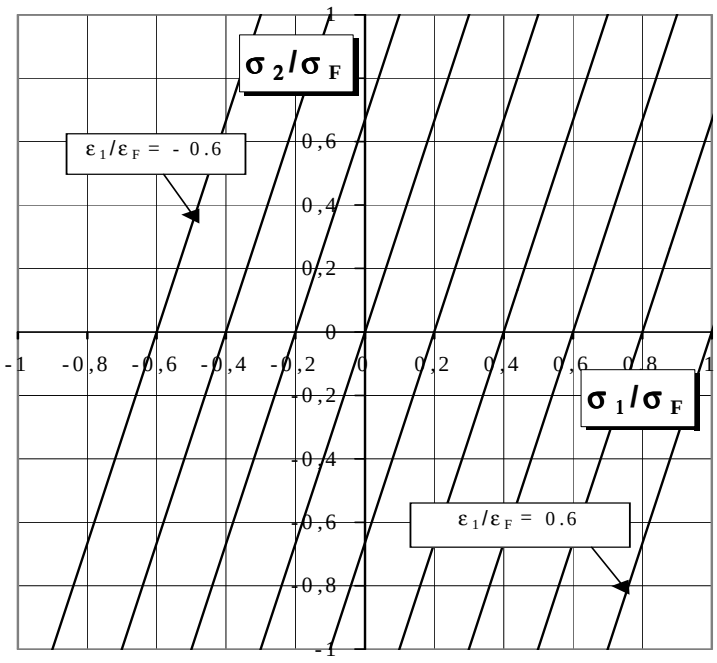

Fig. 9. Contour plots of flexibility for ε_1, biaxial plane stress situation in a material point according to Hooke's law. $\varepsilon_1 \in$ [-0.6 to 0.6] ε_F , $\Delta\varepsilon_1 = 0.2\ \varepsilon_F$.

Results showing the non-linear response of the plate are presented in Fig. 10, 11 and 12. These results include imperfections and geometric non-linearity effects. Conceptually, these results may be considered as material properties of a macro material point, i.e. the plate as a whole.

It was found most convenient to present the results as contour plots in the form of flexibility curves. This was due to the non-linear finite element code ABAQUS(1994) which was most conveniently run in a displacement control mode with prescribed straight edges. The ABAQUS model had a mesh of 20x20 using thin shell elements S9R5.

The non-linear macro results are presented in Fig.10 for the considered near geometrically perfect plate square plate ($q_{10} = 0.01$). It is seen that the perturbation solution follows very accurately the closed form solution. In the figure the closed form solution and the perturbation solution are indistinguishable. The perturbation solution is based on a second order expansion together with small increments of the arc length parameter η of the order of 0.01. In the same figure are added results from the ABAQUS analyses. It is shown that the ABAQUS results follows very closely the closed form solution up to certain point for then to suddenly change direction. This change of direction of the equilibrium path is associated with change of buckling mode from a single half wave in transverse direction to three halfwaves. This phenomenon is referred to as mode snapping in the literature, and the present single degree of freedom model is not capable of predicting such change of modes.

From a structural point of view, Fig.10 illustrates the sudden change of in-plane flexibility/stiffness against relative edge shortening ε_1 as soon as the stability boundary

(eigenvalues) is crossed. It is observed that the density is increased and direction turned of the potential curves beyond the buckling boundary. Below the buckling boundary (lower left part of diagram) the loads are in tension in both directions and the contour lines describes Hooke's law. This prediction is consistent with the simple solution given in eq.(129), which gives a 50% stiffness reduction in the postbuckling region together with a negative Poisson effect.

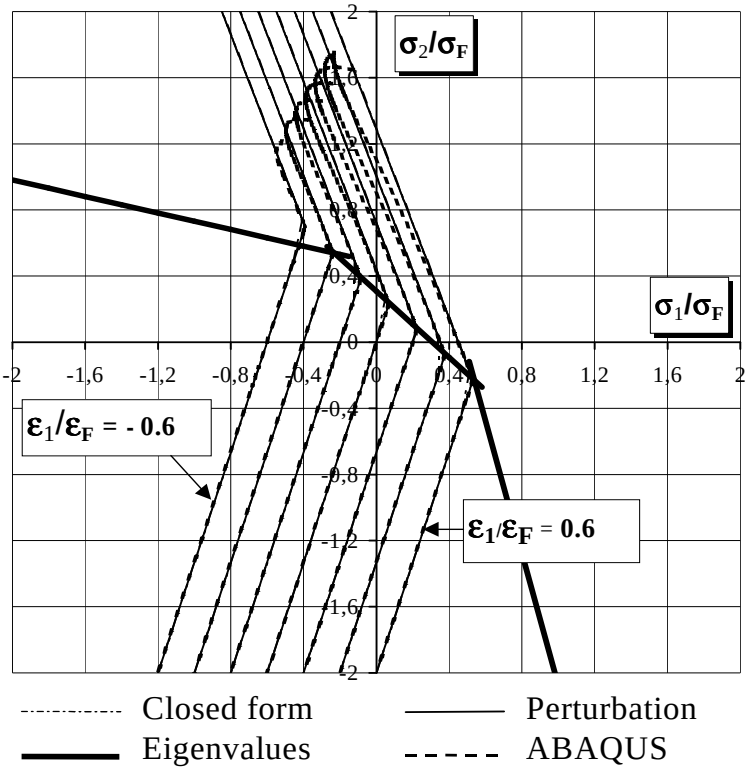

Fig. 10. Contour plots of flexibility curves for a biaxially loaded, geometrically perfect square plate, $\varepsilon_1 \in$ [-0.6 to 0.6] ε_F , $\Delta\varepsilon_1 = 0.2\ \varepsilon_F$. Comparison between closed form solution, numerical perturbation solution and non-linear finite element results/ABAQUS.
Square plate with dimensions, a = b =1000 mm, t =12 mm, δ = 0.12 mm.

In Fig.11 results are presented for the same plate, but with a geometrical imperfection amplitude of δ = 6 mm (q_{10} = 0.5) and with the load axes limiting the interesting response to stay within the yield stress. It is shown that the numerical perturbation procedure follows very accurately the closed form solution and ABAQUS results, and the curves are almost coincident.

From a structural point of view it is seen that the effect of increasing the geometrical imperfection is to give a more gradual transition between the prebuckling flexibility and postbuckling flexibility around the buckling boundary.

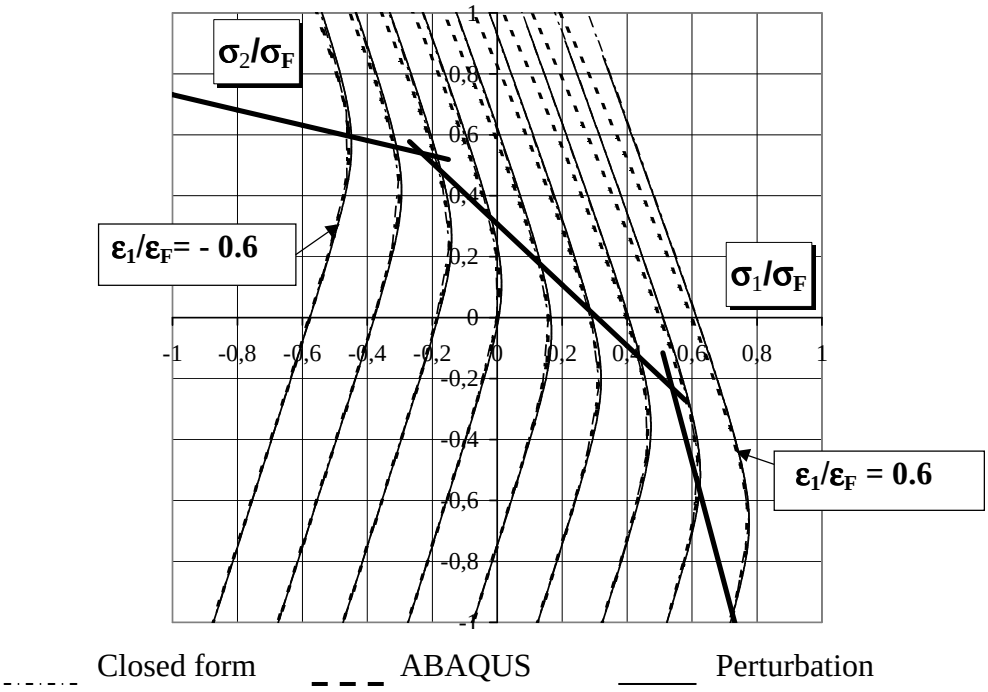

Fig. 11. Contour plots of flexibility curves for a biaxially loaded, geometrically imperfect square plate, $\varepsilon_1 \in [-0.6 \text{ to } 1.0]\varepsilon_F$, $\Delta\varepsilon_1 = 0.2\varepsilon_F$. Comparison between closed form solution, numerical perturbation solution and non-linear finite element results/ABAQUS.
Square plate with dimensions, a = b =1000 mm, t =12 mm, δ = 6 mm.

As discussed in the text, contour plot of stiffness properties is the inverse of the flexibility. For the purpose of being complete the stiffness variations for the load σ_1 in the shortening space (ε_1, ε_2), of the example in Fig.11, is presented in Fig.12. This figure also shows that the perturbation solution coincides with the closed form solution and in Fig.12 it is not possible to distinguish between them.

As seen in Fig.12 the potential stiffness curves are more spread in the postbuckling region (upper right part) than in the tension region (lower left part) where they also are oriented in the opposite direction. This illustrates the reduced stiffness properties for compressive loads and a change of the Poisson effect from positive in the tension region to negative in the compressive region.

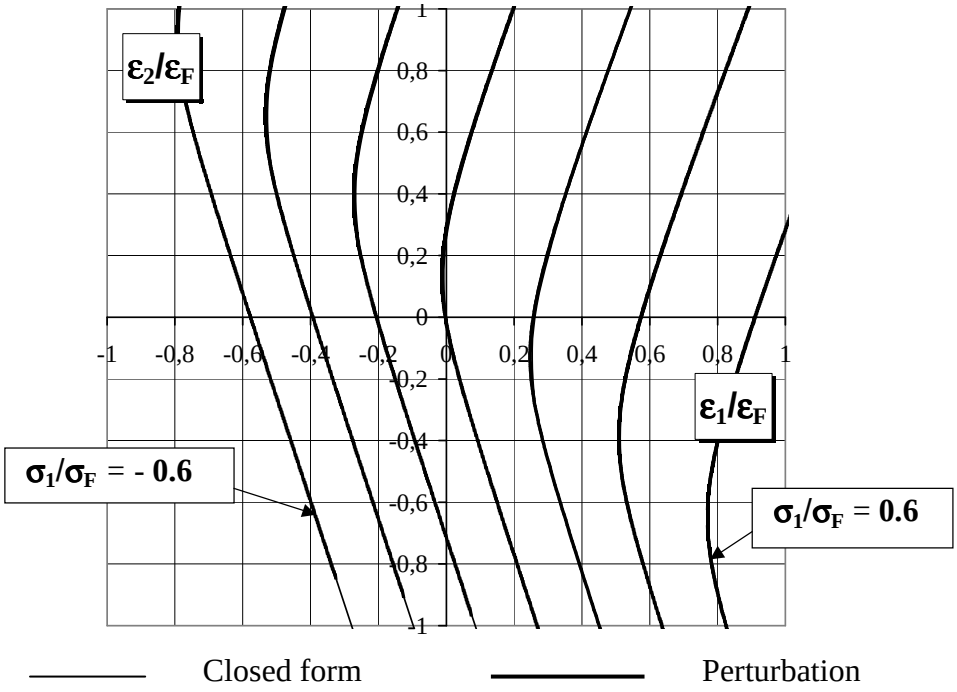

Fig. 12. Contour plots of stiffness curves for a biaxially loaded, geometrically imperfect square plate, $\sigma_1 \in [-0.6 \text{ to } 1.0]\ \sigma_F$, $\Delta\sigma_1 = 0.2\ \sigma_F$. Comparison between closed form solution, numerical perturbation solution.
Square plate with dimensions, a = b =1000 mm, t =12 mm, δ = 6 mm.

5. CONCLUSIONS

The general perturbation method for discrete systems, developed for the purpose of analysing stability properties of structures, is described. In the present work the main emphasis is on tracing the complete non-linear equilibrium path from the unloaded state to limit points and with subsequent assessment of the initial postbuckling region of geometrically imperfect structures. The perturbation method is applied up to a second order expansion of the equilibrium path and the procedure is embedded in an incremental scheme. The second order expansion is adopted as a substitute for the standard equilibrium control applied in more traditional incremental numerical methods. The arc length concept for multiple loads is introduced for passing limit and snap back points along the equilibrium surface. The direct arc length method, applied in a perturbation scheme, is discussed in relation to Riks' method, which is a method that is accepted as one of the most efficient in numerical analysis of instability problems.

The incremental perturbation scheme is applied to a simple single degree of freedom system of a biaxially loaded plate, and it is shown that the numerical results very closely compare with a closed form solution. Included are also results obtained using the non-linear finite element code ABAQUS. The present example is rather simple and does not give conclusive answers on the efficiency of the present proposed numerical scheme. However, the incremental perturbation scheme presented here has been developed with the main purpose of

solving buckling problems that can be described with relatively few degrees of freedom. From this point of view the method works very satisfactory and in Steen(1999) the procedure is applied to a more complex plate model. In that model the non-linear interactive response between local and overall buckling of stiffened panels is addressed.

Properties are shown for a biaxially loaded unstiffened plate as a specific example. The stiffness and flexibility properties are presented as contour plots. This way of showing the results gives a new understanding of the actual buckling process under multiple loads and it embrace a lot of information into one diagram. The contour plots can be interpreted as an illustration of the macro material concept in the sense that it includes both the material and geometrical non-linear behaviour of the whole panel into one diagram.

From an overall point of view, an isolated flat panel in a large structure may be seen as macro material and the change of in-plane stiffness properties due to geometrical imperfections, residual stresses, lateral pressure and buckling behaviour can be all included in the macro material description. The results emerge as orthotropic material parameters, which can subsequently be used as input material properties in large linear finite element models e.g. of ship hulls. This approach provides a more realistic global redistribution of the stresses in the structure than that provided by the normal assumption of linear isotropic material properties according to Hooke's law used in standard linear analyses.

Acknowledgements
The continuos support from dr. S.Valsgård and G.Holtsmark, DNV and professor J.Hellesland, University of Oslo, is highly appreciated. Patient assistance by my colleagues Eirik Andreassen, Gaute Storhaug, Tom K. Østvold and Anders B. Engelsen at DNV is also highly appreciated.

6. REFERENCES

ABAQUS, Version 5.5, User's Manual, Hibbitt, Karlsson & Sorensen, Inc. 1995, U.S.A.

Benito, B. and Sridharan, S. (1985). "Interactive buckling analysis with finite strips". International Journal for Numerical Methods in Engineering, Vol.21, 145-161.

Budiansky, B. and Hutchinson, J.W. (1964). "Dynamic buckling of imperfection-sensitive structures", Proc. 11th IUTAM Congress, Münich.

Budiansky, B. and Amazigo, J.C. (1968). "Initial postbuckling behaviour of cylindrical shells under external pressure", J. Math. Phys., Vol.47,

Budiansky, B. (1969)."Postbuckling behaviour of cylinders in torsion" in Theory of Thin Shells. Edited by Niordson, F.J.Springer-Verlag,

Budiansky, B. (1974).”Theory of buckling and post-buckling behaviour of elastic structures”, in Advances in Applied Mechanics, Vol.14, Academic Press.

Carrera, E, (1994). “A study on arc-length type methods and their operation failures illustrated by a simple model”, Computers & Structures, Vol.50.

Chilver, A.H. (1967).” Coupled modes of elastic buckling”. J.Mech.Phys.Solids, Vol.15.

Crisfield, M.A and Shi, J. (1991) “A review of solution procedures and path-following techniques in relation to the non-linear finite element analysis of structures”. Published in Non-linear Computational Mechanics, Editors: P. Wriggers and W.Wagner, Springer-Verlag,

Huseyin, K. (1975).”Nonlinear theory of elastic stability”, Noordhoff International Publishing, Leyden.

Hutchinson, J.W. (1967). “Initial postbuckling behaviour of toroidal shell segments”, Int.J.Solids and Structures, Vol. 3.

Hutchinson, J.W. (1968). “Buckling and initial postbuckling behaviour of oval cylindrical shells under axial compression, J.Appl. Mech.,Vol.35.

Hutchinson, J.W. and Koiter, W.T. (1970). “Postbuckling theory”, Appl. Mech. Rev.,Vol 23.

Johns, K.C. and Chilver, A.H. (1971). ”Multiple path generation at coincident branching points”, Tech. Report No.KJ-1, University College, London

Koiter, W.T. (1945). “On the stability of elastic equilibrium (in Dutch with English summary)”, Thesis, Delft, H.J. Paris, Amsterdam. English translation: Air Force Flight Dyn.Lab.Tech.Rep.AFFDL-TR-70-25, Stanford University, Dept. of Aeronautics and Astronautics, U.S.A., 1970.

Lanco, A. D. and Garcea, G. (1996). “Koiter’s analysis of thin-walled structures by a finite element approach”. International Journal for Numerical Methods in Engineering, Vol.39, pp. 3007-3031.

Marguerre, K. (1938). “Zur theorie der gekrümmten platte grosser formeändrug”, Proceedings of the 5^{th} international congress for applied mechanics, p. 93-101.

Riks, E. (1972). “The application of Newton’s method to the problem of elastic stability”, Journal of Applied Mechanics, Vol. 39, pp.1060-1066.

Riks, E. (1979). “An incremental approach to the solution of snapping and buckling problems”, Int. J. Solids and Structures, Vol. 15, pp. 529-551.

Sewell, M.J. (1965). “The static perturbation technique in buckling problems”. J.Mech.Phys. Solids,**13**, pp.247-265.

Sewell, M.J. (1968). “A general theory of equilibrium paths through critical points”. I. Proc.Roy.Soc.A., **306**, pp.201-223.

Steen, E, (1984). “Simplified ultimate strength evaluation of geometrically imperfect and damaged plates subjected to multiple loads”, DNV Report no. 84-3663, Høvik, Norway.

Steen, E, (1989). “Elastic buckling and postbuckling of eccentrically stiffened plates”, Int.J.Solids and Structures, Vol.25.

Steen, E, (1999). “Buckling of stiffened plates using a Shanley model approach”, Research Report in Mechanics, No. 99-1, Mechanics Division, Department of Mathematics, University of Oslo.

Steen, E and Andreassen, E. (1995-I). “Buckling of stiffened plates under combined loads. PP2: Basic Theory Development CSA-2”, DNV Report No.95-0198, Høvik, Norway.

Steen, E and Andreassen, E. (1995-II). “Buckling of stiffened plates under combined loads. PP2: Detailed Theory Development CSA-2”, DNV Report No.95-0479, Høvik, Norway.

Stoll, F. (1994). “An implementation of solution strategies for the analysis of complex non-linear equilibrium behaviour”, Int. J. Non-Linear Mechanics. Vol. 29, No.2, pp.109-122.

Stoll, F. (1994). “Analysis of the snap phenomenon in buckled plates”, Int. J. Non-Linear Mechanics. Vol. 29, No.2, pp.123-138.

Supple, W.J. (1967).”Coupled branching configurations in the elastic buckling of symmetric structural systems”. Int.J.Mech. Sci.,Vol.9.

Thompson, J.M.T. (1965). “Discrete branching points in the general theory of elastic stability”. J.Mech.Phys. Solids,**13**, pp.295-310,.

Thompson, J.M.T. and Hunt, G.W. (1973). “A general theory of elastic stability”, John Wiley & Sons, Great Britain.

Thompson, J.M.T. and Hunt, G.W. (1984). “Elastic Instability Phenomena”, John Wiley & Sons, Great Britain.

Van Erp. G.M and Menken, C.M. (1991). “Initial post-buckling analysis with the spline finite-strip method”. Computers and Structures, Vol.40, 1193-1201.

Von Karman, T. (1910). ”Festigkeitsprobleme in maschienbau”. Encyklopädie der matematischen Wissenschafen, Vol.IV,4,Chap.27,pp.349.

Washizu, Kyuichiro, (1975). “Variational methods in elasticity and plasticity”, Pergamon Press, Second Edition, Bath, Great Britain.

Wempner, G. (1973). “Mechanics of solids with applications to thin bodies”, McGraw-Hill, Inc., U.S.A.

7. NOTATION

Latin letters

a	Plate length in x_1 direction
b	Plate length in x_2 direction
t_p	Plate thickness
t	Pseudo time parameter
w	Plate deflection normal to plate plane, used here as amplitude
p	Lateral uniform pressure acting normal to plate
g_u	Buckling boundary function ($g_u = 0$; buckling boundary equation)
ℓ_1	Wave length of buckling pattern in x_1 direction ($\ell_1 = a/m$)
ℓ_2	Wave length of buckling pattern in x_1 direction ($\ell_2 = b/n$)
E	Youngs' modulus
ν	Poisson's' ratio
m	Number of half waves in x_1-direction
n	Number of half waves in x_2-direction
M	Total number of degrees of freedom
K	Total number of independent loads (or edge displacements)
x_1,x_2,x_3	Rectangular coordinate system

Greek symbols

σ_F	Yield stress, (only used for scaling purposes in this report)
σ_α	Average membrane stress
σ_1	Average membrane stress in x_1 direction, positive in compression
σ_2	Average membrane stress in x_2 direction, positive in compression
ε_α	End-shortening of plate edges
ε_1	End-shortening of plate edges (av. strain), x_1 direction, positive in compression
ε_2	End-shortening of plate edges (av. strain), x_2 direction, positive in compression
Λ	General load parameter, non-dimension
Λ_α	General load parameter, non-dimension
Δ_α	General displacement parameter, non-dimension
Δ	Symbol for incremental property
δ	Initial plate imperfection amplitude, stress free
η	Perturbation parameter, arc length along equilibrium curve
η_α	Perturbation parameter, arc length along equilibrium surface, multiple dimensional
$\delta^{\alpha\beta}$	Kronecker delta

Vector, matrix, tensor symbols

f_i	Equilibrium functions ($f_i = 0$; equilibrium equations)
q_i	General degree of freedom parameter, non-dimension
q_{i0}	Initial general degree of freedom parameter, stress free, non-dimension
d_i	Element in column matrix, see eq.(43)
c_i^{α} c_β^{α}	Directional cosines of equilibrium path in load-deflection space, see eq.(17)
∇	Symbol for vector gradient
$\mathbf{i}$	Unit vector in direction of ant load σ_α, see eq.(71), presentation of stiffness
$\mathbf{i}_\beta$	Unit vector in direction of any ε_α , see eq.(71), presentation of stiffness
$\mathbf{i}_p$	Unit vector in direction p , see eq.(71), presentation of stiffness
$\mathbf{r}_\alpha$	Radius vector in (σ_α, ε_1, ε_2,.., ε_K, p) space, presentation of stiffness

$\mathbf{t}_\alpha$	Tangent vector in (σ_α, ε_1, ε_2,.., ε_K, p) space, presentation of stiffness
$\mathbf{t}_\varepsilon$	Tangent vector in (ε_1, ε_2,.., ε_K, p) space along prescribed load history
$\boldsymbol{\kappa}_\alpha$	Curvature vector in (σ_α, ε_1, ε_2,.., ε_K, p) space, presentation of stiffness
$\left\|\boldsymbol{\kappa}_\alpha\right\|$	Length of curvature vector κ_α, see eq.(75)
$\mathbf{n}_\alpha$	Unit vector in (σ_α, ε_1, ε_2,.., ε_K, p) space along curvature vector κ_α
$\mathbf{i}_\Lambda$	Unit vector in solution space along Λ axis
$\mathbf{i}_i$	Unit vector in solution space along q_i axis
$\dot{\mathbf{x}}$	General solution vector, see eq.(38)
$\dot{\mathbf{x}}_+$	First solution vector, see eq.(44a)
$\dot{\mathbf{x}}_-$	Second solution vector, see eq.(44b)
$\dot{\mathbf{q}}$	Displacement vector, see eq.(41)
$\mathbf{f} \equiv \left[f_i{}^j\right]$	First order matrix, see eq.(41)
$\mathbf{f}^\Lambda \equiv \left[f_i{}^\Lambda\right]$	First order column matrix, see eq.(41)
$\mathbf{J} \equiv \left[\partial\varepsilon_\alpha / \partial\eta_\beta\right]$	Jacobian matrix , see eq.(100a), inverted see eq.(102a)
$\mathbf{J}^p \equiv \left[\partial\varepsilon_\alpha / \partial p\right]$	Jacobian column matrix , see eq.(100b)
$\dot{\Lambda}_\pm$	Two solutions for the first order load rate, see eq.(44c)
$K_{\alpha\beta}$	First order stiffness coefficients, see eq.(52)
$K_{\alpha\beta\delta}$	Second order stiffness coefficients, see eq.(52)
$C_{\alpha\beta}$	First order in-plane stiffness coefficients of flat plates, see eq.(62)
$C_{\alpha p}$	First order in-plane stiffness coefficients of flat plates, see eq.(62)
$C_{\alpha\beta\delta}$	Second order in-plane stiffness coefficients of flat plates, see eq.(62)
$C_{\alpha\beta p}$	Second order in-plane stiffness coefficients of flat plates, see eq.(62)
$C_{\alpha pp}$	Second order in-plane stiffness coefficients of flat plates, see eq.(62)
$M_{\alpha\beta}$	First order in-plane flexibility coefficients of flat plates, see eq.(66)
$M_{\alpha p}$	First order in-plane flexibility coefficients of flat plates, see eq.(66)
$M_{\alpha\beta\delta}$	Second order in-plane flexibility coefficients of flat plates, see eq.(66)
$M_{\alpha\beta p}$	Second order in-plane flexibility coefficients of flat plates, see eq.(66)
$M_{\alpha pp}$	Second order in-plane flexibility coefficients of flat plates, see eq.(66)
$\Im_\alpha$	Compatibility function, see eq.(53)
$\Re_\alpha$	Inverse compatibility function, see eq.(58)

Subscripts and superscripts

i, j, k,…	Dummy indices, Latin letters used as subscript and superscript, range 1,2,,..,M
α, β, γ, λ,…	Dummy indices, Greek letters used as subscript and superscript, range 1,2,,..,K (K-1)
s	Evaluated at any state I_s
m	State along prescribed piecewise linear load history in load or displacement space

Notation for derivatives

∂	Partial derivative symbol
$\dot{q}_i = \frac{\partial q_i}{\partial \eta}$	Path derivatives with respect to arc length η
$\dot{\sigma}_\alpha = \frac{\partial \sigma_\alpha}{\partial \eta}$	Path derivatives of load parameter
$\dot{\varepsilon}_\alpha = \frac{\partial \varepsilon_\alpha}{\partial \eta}$	Path derivatives of end-shortening parameter
$\dot{\Lambda} = \frac{\partial \Lambda}{\partial \eta}$	Path derivatives of load, non-dimensionless parameter

$$q_i{}^{\gamma} = \frac{\partial q_i}{\partial \eta_\gamma} \qquad q_i{}^{\gamma\lambda} = \frac{\partial^2 q_i}{\partial \eta_\gamma \partial \eta_\lambda}$$

$$f_i{}^{j} = \frac{\partial f_i}{\partial q_j} \qquad f_i{}^{\alpha} = \frac{\partial f_i}{\partial \eta_\alpha}$$

$$f_i{}^{jk} = \frac{\partial f_i}{\partial q_j \partial q_k} \quad f_i{}^{j\alpha} = \frac{\partial f_i}{\partial q_j \partial \eta_\alpha} \quad f_i{}^{\alpha\beta} = \frac{\partial f_i}{\partial \eta_\alpha \partial \eta_\beta}$$

$$\Lambda_\alpha{}^{\beta} = \frac{\partial \Lambda_\alpha}{\partial \eta_\beta} \qquad \Lambda_\alpha{}^{\beta\gamma} = \frac{\partial \Lambda_\alpha}{\partial \eta_\beta \partial \eta_\gamma}$$

$$\varepsilon_\alpha{}^{\gamma} = \frac{\partial \varepsilon_\alpha}{\partial \eta_\gamma}$$

$$\sigma_\alpha{}^{\gamma} = \frac{\partial \sigma_\alpha}{\partial \eta_\gamma}$$

$$p^{\gamma} = \frac{\partial p}{\partial \eta_\gamma}$$

$$\eta_\gamma{}^{\alpha} = \frac{\partial \eta_\gamma}{\partial \varepsilon_\alpha}$$

$$\eta_\gamma{}^{p} = \frac{\partial \eta_\gamma}{\partial p}$$